Fluctuation and correlation effects in a charged surface immersed in an electrolyte solution

A. W. C. Lau
Department of Physics, Florida Atlantic University, Boca Raton, Florida 33431, USA
(Received 16 July 2007; published 22 January 2008)

We explore correlation and fluctuation effects in an overall neutral system consisting of a single homogeneously charged planar surface with both the counterions and coions distributed on both sides of the surface. Using a field-theoretic formulation, we compute the one-loop correction to the electrostatic potential, to the ion densities, to the surface tension, and to the surface free energy. From the asymptotic behavior of the electrostatic potential, we obtain an exact expression for the effective surface charge density, which can become negative, indicating charge inversion. Furthermore, we find that the ion distributions can be substantially different from the mean-field ion densities. In particular, the counterion density, at high couplings, develops a minimum at some intermediate distances, larger than the Gouy-Chapman length, away from the charged surface, whereas the coion density develops a maximum, whose values can be greater than the counterion density. Therefore, the coions develop a second layer. Moreover, the one-loop correction always lowers the electrostatic contributions to the surface tension and at high couplings, the surface tension may become negative.

DOI: 10.1103/PhysRevE.77.011502 PACS number(s): 82.70.−y, 61.20.Qg, 05.70.−a

I. INTRODUCTION

Electrostatic interaction plays an important role in many biological problems and in colloidal science that involve macroions in aqueous solutions [1]. The macroions may be charged membranes [2], colloidal particles [3], or polyelectrolytes such as DNA [4]. The traditional description for these charged systems relies on the mean-field Poisson-Boltzmann (PB) theory, which fails for highly charged macroions or in the presence of multivalent counterions [5–10]. In particular, it cannot account for such striking phenomena as DNA condensation [11,12], charge inversion [7,13–16], and like-charge attraction [17–21]. In the past couple of decades, many theoretical approaches have been proposed in an attempt to go beyond the mean-field theory (for recent comprehensive reviews, see Refs. [8–10]). These include the integral-equation approach [5,9,22–24], the field-theory formulation [25–28], the heuristic Wigner crystal approach [29,30], and more recently, the strong-coupling theory [6,31]. While most of the recent progress has been made on counterion-only systems [31–33], correlation effects in systems with added salt cannot be undermined since in realistic experimental situations, there is always a finite amount of added salt. In fact, water itself may be considered an electrolyte solution because of the finite degree of dissociation of water molecules. The interplay between three different length scales in the problem—the Debye screening length, the Gouy-Chapman length, and the Bjerrum length—makes correlation effects far richer than the counterion-only systems. Moreover, a number of recent experiments on charged systems with finite salt concentrations are carried out in a regime where correlation effects might be important [13,14,19–21]. Therefore, it is worthwhile to understand correlation effects in charged surfaces immersed in an electrolyte solution.

Some aspects of correlation effects of charged surfaces in salt solutions have been investigated using different methods in the past. In Ref. [23], the ion-ion correlation function and the potential of mean force for a single charged hard wall in contact with an electrolyte solution were discussed. The ion-ion correlation function is equivalent to the Green's function, which represents the electrostatic interaction between two test charges taking in account of the presence of the counterions and coions. Attard *et al.* [24] computed the interaction free energy of two similarly charged hard walls with symmetric electrolyte in between, at the level of Debye-Huckel closure, which is equivalent to the one-loop calculation here, and from the behavior of the pressure at the infinite separation, an analytical expression for the effective charge of the charged surface was obtained [15]. Using the Wigner crystal approach, Shklovskii argued that correlation effects lead to charge inversion of a charged surface [7,29]. The phenomenon of charge inversion has also been studied numerically using the hypernetted-chain approximation [16]. In addition, these calculations, as well as a recent simulation [34], revealed that the formation of a second layer of coion adjacent to the counterions layer near the charged surface.

In this paper, we carry out a comprehensive study of correlation effects using a field theoretical formulation and provide a unified treatment for all the phenomena mentioned above. Our system consists of a charged surface immersed in an electrolyte solution. We assume that the surface is permeable to ions, and thus the counterions and the coions are distributed on both sides of the surface. This system may be a good model for charged membranes, and in particular, for those that contain ion pumps allowing ions to pass freely; the latter systems are of current theoretical interest [35]. In addition to solving for the Green's function for the system, we compute the electrostatic potential, the ion distributions, the surface tension, and the surface free energy, all to one-loop order. From the asymptotic behaviors of the electrostatic potential, we obtain an exact expression for the effective surface charge density to one-loop order. Our expression is different from that of Attard *et al.* [24], although qualitatively they exhibit similar behavior, with one notable difference: in the limit of vanishing surface charge, the expression of Attard *et al.* [24] predicts that the effective charge is renormal-

ized by a finite amount, whereas our expression predicts that the effective charge is *not* renormalized (correlation effects comes in only at the second order in the expansion of vanishing charge). At higher couplings, we find that the effective charge becomes negative, indicating charge inversion. Furthermore, we find that the ion distributions can be substantially different from the mean-field density. Particularly, the counterion density develops a minimum at some intermediate distance greater than the Gouy-Chapman length, and the coion density forms a second layer. The latter result has been observed in a recent simulation [34]. Finally, we compute the free energy analytically and extract the electrostatic contribution to the surface tension, which becomes negative at high couplings.

This paper is organized as follows. In Sec. II, we begin with a brief presentation on the formulation of the field theory for an overall neutral system consisting of a charged surface with mobile ions of both signs, distributed on both sides of the surface. In addition, in Sec. II A, we show that the PB theory can be derived as a saddle-point approximation of the field theory, and we improve upon this approximation by performing a loop expansion, which captures correlation effects systematically. We obtain formal expressions for the electrostatic potential, the ion distributions, the grand potential, and the free energy, all at the one-loop level. In Sec. II B, we briefly review the main features of the mean-field PB theory of our system. In Sec. III, we investigate fluctuation effects in detail. In Sec. III A, we construct the Green's function, which is a central quantity for evaluating various physical quantities at one loop, and we also discuss the physics associated with it: the self-energy of an ion and the interaction potential between two ions near the charged surface. In Sec. III B, we obtain an explicit expression for the one loop correction to the electrostatic potential, and discuss charge renormalization of the surface at one loop. In Sec. III C, we discuss ion distributions at the one loop level. In Sec. III D, we compute the grand potential and the free energy at one-loop, and discuss, in particular, the electrostatic contribution to the surface tension of the charged surface at one-loop. This paper concludes in Sec. IV with a discussion of the validity of the one-loop expansion. Technical details are presented in the Appendixes.

II. FIELD THEORY FORMULATION

In this section, we briefly set up the field theory for a system consisting of a charged surface with counterions and coions distributed on both sides of the surface. For a more elaborate discussion on the derivation of the field theory, see Refs. [26,36]. One of the advantages of a field theory formulation for charged systems is that it facilitates systematic perturbative calculations to investigate correlation effects, and it allows, potentially, the immediate application of all of the powerful techniques of field theory, such as the renormalization group and nonperturbative methods, to study charged systems.

Consider a system that consists of N_- pointlike particles of charge $-Z_-e$ and N_+ pointlike particles of charge $+Z_+e$, as well as a single uniformly charged surface with a negative surface charge density of $\sigma(\mathbf{x}) \equiv -en_f(\mathbf{x}) = -en_0\delta(z)$ [see Fig. 1]. The ions are distributed on both sides of the surface. We assume that both sides have the same dielectric constant ϵ. In order to have a meaningful thermodynamic limit, the system must be neutral; therefore, we impose the charge neutrality condition, which can be written as

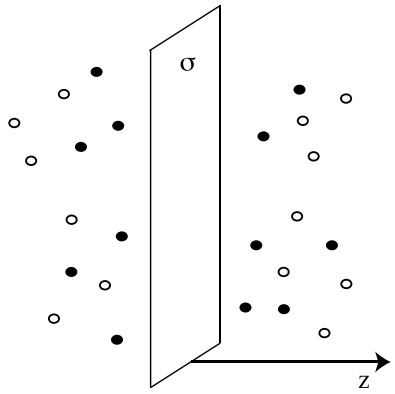

FIG. 1. A single charged plate in salt solution. The system is symmetric with respect to $z=0$. Without the loss of generality, the charged plate is assumed to have a negative surface-charge density $\sigma=-en_0$, with counterions (solid circles) and coions (open circles) present on both sides of the plate. It is assumed that the dielectric constants are the same on both sides of the plate.

$$-Z_-eN_- + Z_+eN_+ - en_0\mathcal{A} = 0, \tag{1}$$

where $\mathcal{A}$ is the area of the plane. The electrostatic energy of the system may be written as

$$\beta E_{N_+,N_-} = \sum_{j>k}^{N_+} \frac{Z_+^2 \widetilde{l_B}}{|\mathbf{x}_j^+ - \mathbf{x}_k^+|} + \sum_{j>k}^{N_-} \frac{Z_-^2 \widetilde{l_B}}{|\mathbf{x}_j^- - \mathbf{x}_k^-|} - \sum_{j=1}^{N_+}\sum_{k=1}^{N_-} \frac{Z_+Z_- \widetilde{l_B}}{|\mathbf{x}_j^- - \mathbf{x}_k^+|} - Z_+\sum_j^{N_+} \phi(\mathbf{x}_j^+) + Z_-\sum_j^{N_-} \phi(\mathbf{x}_j^-), \tag{2}$$

for a set of positive charges located at $\mathbf{x}_i^+$ and a set of negative charges located at $\mathbf{x}_i^-$. In Eq. (2), $\beta \equiv 1/(k_BT)$, k_B is the Boltzmann constant, T is the temperature, $\widetilde{l_B} \equiv e^2/(\epsilon k_BT)$ is the Bjerrum length, and

$$\phi(\mathbf{x}) \equiv \widetilde{l_B} \int d^3\mathbf{x}' \frac{n_f(\mathbf{x}')}{|\mathbf{x} - \mathbf{x}'|}, \tag{3}$$

which is the "external" potential induced by the presence of the charged plate. Note that the external charge density $n_f(\mathbf{x})$ is always positive and that the sign convention has already been tacitly imposed in Eq. (2). Introducing the counterion density operator $\hat{\rho}_+(\mathbf{x}) \equiv \sum_{i=1}^{N_+} \delta(\mathbf{x} - \mathbf{x}_i^+)$, the coions density operator $\hat{\rho}_-(\mathbf{x}) \equiv \sum_{i=1}^{N_-} \delta(\mathbf{x} - \mathbf{x}_i^-)$, and the overall charge density operator $\hat{\rho}_c(\mathbf{x}) \equiv Z_+\hat{\rho}_+(\mathbf{x}) - Z_-\hat{\rho}_-(\mathbf{x})$, we can write Eq. (2) as

$$\beta E_{N_+,N_-} = -V_0^+ N_+ - V_0^- N_- - \int d^3\mathbf{x}\hat{\rho}_c(\mathbf{x})\phi(\mathbf{x}) + \frac{\widetilde{l_B}}{2}\int d^3\mathbf{x}\int d^3\mathbf{x}'\frac{\hat{\rho}_c(\mathbf{x})\hat{\rho}_c(\mathbf{x}')}{|\mathbf{x}-\mathbf{x}'|}, \tag{4}$$

where $V_0^{\pm}$ are the bare (infinite) self-energies of the positive and negative ions, respectively. They are defined by

$$V_0^{\pm} \equiv \frac{\widetilde{l_B}Z_{\pm}^2}{2}\int \frac{d^3\mathbf{q}}{(2\pi)^3}\frac{4\pi}{q^2} = \frac{4\pi\widetilde{l_B}Z_{\pm}^2}{2}\int \frac{d^2\mathbf{q}}{(2\pi)^2}\frac{1}{2q}, \tag{5}$$

where in the last line we have integrated out the q_z component. The self-energy arises because Eq. (4) contains terms that are evaluated at $\mathbf{x}=\mathbf{x}'$ and they are absent in Eq. (2). In what follows, we keep the self-energy terms and see how they are canceled at the one-loop level. The partition function for this system is

$$\mathcal{Z}_{N_+,N_-}[\phi] = \frac{1}{N_+!}\left(\prod_i^{N_+}\int\frac{d\mathbf{x}_i^+}{a_+^3}\right)\frac{1}{N_-!}\left(\prod_i^{N_-}\int\frac{d\mathbf{x}_i^-}{a_-^3}\right)e^{-\beta E_{N_+,N_-}}. \tag{6}$$

In order to reformulate Eq. (6) as a field theory, we introduce the chemical potentials μ_+ and μ_- (in units of k_BT) for the positive and negative ions, respectively, and consider the grand canonical partition function

$$\mathcal{Z}_{\mu_+,\mu_-}[\phi] = \sum_{N_-,N_+=0}^{\infty}(e^{\mu_+})^{N_+}(e^{\mu_-})^{N_-}\mathcal{Z}_{N_+,N_-}[\phi]. \tag{7}$$

After performing a Hubbard-Stratonovich transformation [37], we find that Eq. (7) can be written as

$$\mathcal{Z}_{\mu_+,\mu_-}[\phi] = \mathcal{N}_0\int \mathcal{D}\psi e^{-\mathcal{S}[\psi,\phi]},$$

$$\mathcal{S}[\psi,\phi] \equiv \int d^3\mathbf{x}\left\{\frac{1}{2}\psi(\mathbf{x})\left[-\frac{\nabla^2}{4\pi l_B}\right]\psi(\mathbf{x}) - \theta_+ e^{+Z_+[\imath\psi(\mathbf{x})+\phi(\mathbf{x})]} - \theta_- e^{-Z_-[\imath\psi(\mathbf{x})+\phi(\mathbf{x})]}\right\}, \tag{8}$$

where $\mathcal{S}$ is the action functional, $\psi(\mathbf{x})$ is a fluctuating field, which, as we show below, is related to the electrostatic potential of the system, $\mathcal{N}_0$ is the normalization constant, and $\theta_{\pm}\equiv[\exp(\mu_{\pm}+V_0^{\pm})]/a_{\pm}^3$ denotes the fugacity of the ions. The equilibrium average of a given physical quantity is generated by the partition function (8). For example, the equilibrium density distributions for positive and negative ions are given by

$$\langle\hat{\rho}_{\pm}(\mathbf{x})\rangle \equiv \pm\frac{\delta\ln\mathcal{Z}_{\mu_+,\mu_-}[\phi]}{\delta[Z_{\pm}\phi(\mathbf{x})]} = \theta_{\pm}\langle e^{\pm Z_{\pm}[\imath\psi(\mathbf{x})+\phi(\mathbf{x})]}\rangle. \tag{9}$$

Since $\langle\delta\mathcal{S}/\delta\psi(\mathbf{x})\rangle=0$, we have an exact relation

$$\nabla^2\langle\imath\psi(\mathbf{x})\rangle = 4\pi\widetilde{l_B}Z_+\theta_+\langle e^{+Z_+[\imath\psi(\mathbf{x})+\phi(\mathbf{x})]}\rangle - 4\pi\widetilde{l_B}Z_-\theta_-\langle e^{-Z_-[\imath\psi(\mathbf{x})+\phi(\mathbf{x})]}\rangle, \tag{10}$$

which can be interpreted as the Poisson equation from electrostatics.

For simplicity, we consider an asymmetric electrolyte in which the positive ions and negative ions have the same valence $Z_+=Z_-=Z$ but different radii $a_+\neq a_-$. Note that even though the ions have different sizes, finite-ion size effects are not included in the present work. Rescaling the field $\psi\to Z\psi$, the action is given by

$$\mathcal{S}[\psi,\phi] = \frac{1}{l_B}\int d^3\mathbf{x}\left\{\frac{1}{2}\psi(\mathbf{x})[-\nabla^2]\psi(\mathbf{x}) - \Lambda_+ e^{+[\imath\psi(\mathbf{x})+Z\phi(\mathbf{x})]} - \Lambda_- e^{-[\imath\psi(\mathbf{x})+Z\phi(\mathbf{x})]}\right\}, \tag{11}$$

where we have defined $l_B\equiv 4\pi Z^2\widetilde{l_B}$ and $\Lambda_{\pm}\equiv\theta_{\pm}l_B$. Equation (11) is the final form of the action for our system. Note that the transformation $\psi(\mathbf{x})\to\psi(\mathbf{x})+\imath\mu_0$ and $\mu_{\pm}\to\mu_{\pm}\pm\mu_0$ leave the action $\mathcal{S}$ invariant. This invariance simply means that the electrostatic potential is defined up to an arbitrary constant [38]. Note also that the action $\mathcal{S}$ is inversely proportional to l_B. Therefore, l_B may serve as an expansion parameter. In particular, for small l_B, the partition function (8) is dominated by a $\psi(\mathbf{x})$ that corresponds to the maximum of $\mathcal{S}$. This is the saddle-point approximation, which is equivalent to the mean-field Poisson-Boltzmann theory [25,26,36]. The loop expansion, as we detail below, systematically improves on the mean-field theory.

A. One-loop expansion

To systematically investigate correlation effects, we perform a loop expansion on the field theory characterized by Eq. (8) with the action given by Eq. (11), thus extending the formulation of Ref. [26] to the case of a charged surface immersed in an electrolyte solution. For simplicity, we outline and collect results only up to one-loop order; formal expressions for higher loops can be obtained in a straightforward manner.

As noted in Refs. [26,36], once correlation effects are included, the saddle point is shifted from its zero-loop (mean-field) value. This means that there is a nontrivial correction to the electrostatic potential, and that the chemical potentials for the ions must be renormalized at the one-loop level in order to maintain the charge neutrality condition (1). Therefore, we have to perform a double expansion; let us write $\Lambda_{\pm}=\Lambda_{\pm}^{(0)}+\delta\Lambda_{\pm}$ and $\psi(\mathbf{x})=\psi_0(\mathbf{x})+\Delta\psi(\mathbf{x})$, where $\psi_0(\mathbf{x})$ represents the background field, which must be chosen appropriately. Note that $\Delta\psi(\mathbf{x})$ is of the order of $\sqrt{l_B}$: $\Delta\psi(\mathbf{x})\sim\sqrt{l_B}$, while $\delta\Lambda_{\pm}\sim l_B$ at the one-loop level. Putting the above expansions for $\Lambda_{\pm}$ and for $\psi(\mathbf{x})$ into Eq. (11), we find

$$\mathcal{S}[\psi,\phi] = \mathcal{S}[\psi_0,\phi] - \frac{1}{l_B}\int d^3\mathbf{x}\{\delta\Lambda_+ e^{+[\imath\psi_0(\mathbf{x})+Z\phi(\mathbf{x})]} + \delta\Lambda_- e^{-[\imath\psi_0(\mathbf{x})+Z\phi(\mathbf{x})]}\} + \frac{1}{2}\int d^3\mathbf{x}\int d^3\mathbf{x}'\Delta\psi(\mathbf{x})K(\mathbf{x},\mathbf{x}')\Delta\psi(\mathbf{x}') + \mathcal{S}_I, \tag{12}$$

where we have chosen $\psi_0(\mathbf{x})$, at the one-loop level, to obey

$$\nabla^2[\imath\psi_0(\mathbf{x})] - \Lambda_+^{(0)} e^{+[\imath\psi_0(\mathbf{x})+Z\phi(\mathbf{x})]} + \Lambda_-^{(0)} e^{-[\imath\psi_0(\mathbf{x})+Z\phi(\mathbf{x})]} = 0, \tag{13}$$

so that the linear term proportional to $\Delta\psi(\mathbf{x})$ in the expansion of the action $\mathcal{S}$ vanishes identically. In Eq. (12), the operator $K(\mathbf{x},\mathbf{x}')$, coming from the second variations of $\mathcal{S}$, is given by

$$K(\mathbf{x},\mathbf{x}') \equiv \frac{1}{l_B}\{-\nabla_{\mathbf{x}}^2 + \Lambda_+^{(0)} e^{+[\imath\psi_0(\mathbf{x})+Z\phi(\mathbf{x})]} + \Lambda_-^{(0)} e^{-[\imath\psi_0(\mathbf{x})+Z\phi(\mathbf{x})]}\}\delta(\mathbf{x}-\mathbf{x}'), \tag{14}$$

and the interacting part of the action $\mathcal{S}_I$ is given by

$$\mathcal{S}_I = -\int \frac{d^3\mathbf{x}}{l_B}\left\{F(\mathbf{x})[\imath\Delta\psi(\mathbf{x})] + \frac{1}{3!}H(\mathbf{x})[\imath\Delta\psi(\mathbf{x})]^3\right\} + O(l_B), \tag{15}$$

to one-loop order, where $F(\mathbf{x})$ and $H(\mathbf{x})$ are defined by

$$F(\mathbf{x}) \equiv \delta\Lambda_+ e^{[\imath\psi_0(\mathbf{x})+Z\phi(\mathbf{x})]} - \delta\Lambda_- e^{-[\imath\psi_0(\mathbf{x})+Z\phi(\mathbf{x})]}, \tag{16}$$

$$H(\mathbf{x}) \equiv \Lambda_+^{(0)} e^{[\imath\psi_0(\mathbf{x})+Z\phi(\mathbf{x})]} - \Lambda_-^{(0)} e^{-[\imath\psi_0(\mathbf{x})+Z\phi(\mathbf{x})]}. \tag{17}$$

Equation (13) is equivalent to the Poisson-Boltzmann equation. To see this, we define

$$\varphi_0(\mathbf{x}) \equiv \imath\psi_0(\mathbf{x}) + Z\phi(\mathbf{x}) - \frac{1}{2}\ln(\Lambda_-^{(0)}/\Lambda_+^{(0)}), \tag{18}$$

and in term of $\varphi_0(\mathbf{x})$, Eq. (13) becomes

$$-\nabla^2\varphi_0(\mathbf{x}) + \kappa^2 \sinh[\varphi_0(\mathbf{x})] = \frac{l_B}{Z}n_f(\mathbf{x}), \tag{19}$$

which is indeed the nonlinear Poisson-Boltzmann equation with $\kappa^2 \equiv 2\sqrt{\Lambda_+^{(0)}\Lambda_-^{(0)}}$ as the inverse of the Debye screening length squared. Note that the constant $-\frac{1}{2}\ln(\Lambda_-^{(0)}/\Lambda_+^{(0)})$, in Eq. (18) is needed to correctly produce the electrostatic potential in the limiting case in which only counterions are present, but otherwise it is immaterial. In Sec. II B, we will briefly review the salient features of the mean-field theory for this system.

To go beyond the mean-field description at the one-loop level, we must include terms in $\mathcal{S}_I$, Eq. (15), and compute the correction to the electrostatic potential $\Delta\psi(\mathbf{x})$ via $\langle[\imath\Delta\psi(\mathbf{x})]\rangle = \langle[\imath\Delta\psi(\mathbf{x})]e^{-\mathcal{S}_I}\rangle_0$, where $\langle\cdots\rangle_0$ denotes the average with respect to the Gaussian distribution. In particular, the correlation function at zero loop is given by $\langle\Delta\psi(\mathbf{x})\Delta\psi(\mathbf{x}')\rangle_0 = G(\mathbf{x},\mathbf{x}')$, where $G(\mathbf{x},\mathbf{x}')$ is the Green's function, the inverse of $K(\mathbf{x},\mathbf{x}')$: $\int d^3\mathbf{y}K(\mathbf{x},\mathbf{y})G(\mathbf{y},\mathbf{x}') = \delta^3(\mathbf{x}-\mathbf{x}')$. Note that $G(\mathbf{x},\mathbf{x}') \sim l_B$, and therefore, it is not renormalized at the one-loop level. In Sec. III A, we will solve for $G(\mathbf{x},\mathbf{x}')$ explicitly for our system. Evaluating $\langle[\imath\Delta\psi(\mathbf{x})]\rangle$ to one loop, we find a formal expression for it:

$$\langle[\imath\Delta\psi(\mathbf{x})]\rangle_1 = \frac{1}{l_B}\int d^3\mathbf{x}'G(\mathbf{x},\mathbf{x}') \times\left[\frac{1}{2}G(\mathbf{x}',\mathbf{x}')H(\mathbf{x}') - F(\mathbf{x}')\right]. \tag{20}$$

In Sec. III B, we will evaluate $\langle[\imath\Delta\psi(\mathbf{x})]\rangle_1$ explicitly and discuss its relevant physics, such as charge renormalization. By the same token, the ion distributions at one-loop are given by

$$\langle\hat{\rho}_\pm(\mathbf{x})\rangle_1 = \theta_\pm^{(1)} e^{\pm[\imath\psi_0(\mathbf{x})+Z\phi(\mathbf{x})]}\langle e^{\pm\imath\Delta\psi(\mathbf{x})}e^{-\mathcal{S}_I}\rangle_0 = \frac{\kappa^2 e^{\pm\varphi_0(\mathbf{x})}}{2l_B}\left\{1 \pm \langle\imath\Delta\psi(\mathbf{x})\rangle_1 - \frac{1}{2}G(\mathbf{x},\mathbf{x}) + \frac{\delta\Lambda_\pm}{\Lambda_\pm^{(0)}}\right\}. \tag{21}$$

Note that $\delta\Lambda_+$ and $\delta\Lambda_-$, appearing in Eqs. (20) and (21), must be determined in such a way that all the (infinite) bare self-energies $V_0^\pm$ cancel out and that $\langle[\imath\Delta\psi(\mathbf{x})]\rangle_1$ satisfies boundary conditions as imposed by the charge neutrality condition. We will discuss our results for the ion distributions in Sec. III C.

The grand potential $\Omega[\phi]$ is defined by $\Omega[\phi] \equiv -k_BT\ln\mathcal{Z}_{\mu_+,\mu_-}[\phi]$. To one-loop order, we find that it is formally given by

$$\beta\Omega[\phi] = \mathcal{S}[\psi_0,\phi] + \frac{1}{2}\ln\det\hat{\mathbf{K}} - \frac{1}{2}\ln\det[-\nabla_{\mathbf{x}}^2/l_B] - \frac{1}{l_B}\int d^3\mathbf{x}\{\delta\Lambda_+ e^{+[\imath\psi_0(\mathbf{x})+Z\phi(\mathbf{x})]} + \delta\Lambda_- e^{-[\imath\psi_0(\mathbf{x})+Z\phi(\mathbf{x})]}\} + O(l_B), \tag{22}$$

where the second term comes from the "Gaussian" integration over the quadratic order of $\Delta\psi$ in Eq. (12), the third term comes from the normalization constant $\mathcal{N}_0$ in Eq. (8), and the fourth term comes from the expansion of $\Lambda_\pm$ [see Eq. (12)]. Finally, the Helmholtz free energy is related to the grand-canonical potential by

$$\beta F = \beta\Omega[\phi] + \mu_+\int d^3\mathbf{x}\langle\hat{\rho}_+(\mathbf{x})\rangle + \mu_-\int d^3\mathbf{x}\langle\hat{\rho}_-(\mathbf{x})\rangle. \tag{23}$$

In Sec. III D, we will evaluate the grand potential and the free energy for our system to one-loop order explicitly.

B. Mean-field theory

Before discussing fluctuation effects, it is worthwhile to summarize essential features of the mean-field theory, so that we may compare it with fluctuation effects to be discussed in the next section. The solution of the nonlinear Poisson-Boltzmann equation (19) for a single charged plate with $n_f(\mathbf{x}) = n_0\delta(z)$ in a salt solution may be written as [1]

$$\varphi_0(z) = 4\tanh^{-1}e^{-\kappa(|z|+z_0)}, \tag{24}$$

$$= 2 \ln\left[\frac{1+(\sqrt{1+s^2}-s)e^{-\kappa|z|}}{1-(\sqrt{1+s^2}-s)e^{-\kappa|z|}}\right], \tag{25}$$

where z_0 is determined by the boundary condition dictated by Gauss's law at the surface $\varphi_0'(0)=2/\lambda$, which leads to $\sinh(\kappa z_0)=\kappa\lambda\equiv s$, where $\lambda\equiv 4Z/(n_0 l_B)$ is the Gouy-Chapman length, and $s\equiv\kappa\lambda$. Note that s^{-1} is proportional to the bare surface charge density of the plate, n_0. In Eq. (25), z_0 may be interpreted as the length scale over which the counterions are confined: for $s\ll 1$, $z_0\sim\lambda$, while for $s\gg 1$, $z_0\sim\kappa^{-1}$. It is easy to see from Eq. (25) that the potential $\varphi_0(z)$ decays exponentially from the surface with a decaying length set by κ^{-1},

$$\varphi_0(z) = 4(\sqrt{1+s^2}-s)e^{-\kappa|z|} + O(e^{-2\kappa|z|}) \tag{26}$$

for $|z|\to\infty$. Thus, we may define an effective charge of the charged surface as [39]

$$\sigma_{\text{eff}}(s) \equiv 4s\left(\sqrt{1+\frac{1}{s^2}}-1\right). \tag{27}$$

When the bare surface charge is low, $s\gg 1$, $\sigma_s(s)\sim 2/s$, which is proportional to the bare surface charge. This is the Debye-Huckel (DH) regime, where linearization of the PB equation is a good approximation. At high surface charge $s\ll 1$, $\sigma_s(s)\sim 4$, which is independent of the bare surface charge. This is the Gouy-Chapman (GC) regime, where most of the counterions are confined near the surface with a thickness of λ.

From Eq. (9), the ion densities at the mean-field level may be written as

$$\rho_{\pm}^{(0)}(z) = \theta_{\pm}^{(0)} e^{\pm[\imath\psi_0(\mathbf{x})+Z\phi(\mathbf{x})]} = \frac{\kappa^2}{2l_B} e^{\pm\varphi_0(z)} = \frac{\kappa^2}{2l_B}\left[\frac{1\pm(\sqrt{1+s^2}-s)e^{-\kappa|z|}}{1\mp(\sqrt{1+s^2}-s)e^{-\kappa|z|}}\right]^2. \tag{28}$$

It is easy to verify that the charge neutrality condition (1) expressed, at the mean-field level, as

$$\int d^3\mathbf{x}[Z_+ e\rho_+^{(0)}(\mathbf{x}) - Z_- e\rho_-^{(0)}(\mathbf{x})] = e n_0 \mathcal{A} \tag{29}$$

is satisfied. In the DH regime, $s\gg 1$, the ion densities decay exponentially to their bulk values of $\kappa^2/(2l_B)$. In the GC regime $s\ll 1$, the counterion density reduces to the familiar profile of $\rho_+^{(0)}(z)=2/[l_B(|z|+\lambda)^2]$. Note that at the mean-field level, the electrostatic potential (25) and the ion densities (28) at the charged surface satisfy the contact value theorem [40], which in the case of added salt may be written as $\rho_+^{(0)}\times(0)+\rho_-^{(0)}(0)-\kappa^2/l_B=\varphi_0'(0)/(l_B\lambda)$, where the left-hand side represents the (excess) pressure arising from the ion distributions at the surface and the right-hand side represents the electrostatic stress. Therefore, the contact value theorem is a statement that the pressure at the charged surface equals to the pressure in the bulk. However, as we see below in Sec. III C, the ion distributions and the electrostatic potential for our system at the one-loop level no longer obey the contact value theorem, since it is an exact relation only for a charged hard wall [26,40] which is impermeable and impenetrable to ions. Note that our charged surface is assumed to be permeable to ions.

At the mean-field level, the grand potential is simply given by the zero-loop action $\beta\Omega_0[\phi]=\mathcal{S}[\psi_0,\phi]$, which has the form $\beta\Omega_0[\phi]=-p_0\mathcal{V}+\gamma_0(s)\mathcal{A}$, as expected for an interfacial problem [41]. The pressure (in units of k_BT) is given by $p_0=\kappa^2/l_B=2c_s$, from which we identify $\kappa^2=2c_s l_B$, where c_s is the average salt concentration. The surface tension $\gamma_0(s)$ is given by [42]

$$\gamma_0(s) = \frac{2}{l_B\lambda}\ln(\Lambda_-^{(0)}/\Lambda_+^{(0)}) - \frac{8}{l_B\lambda}(\sqrt{1+s^2}-s) + \frac{8}{l_B\lambda}\ln\left(\frac{1+\sqrt{1+s^2}}{s}\right). \tag{30}$$

Apart from the first factor, this agrees with the expression given in Refs. [38,43]. Note that $\gamma_0(s)$ is always positive and diverges as $\gamma_0(s)\sim -\ln s$ as $s\to 0$, i.e., $n_0\to\infty$. However, in order to produce the electrostatic contribution to the surface tension for the counterion-only case $\gamma_0=-2n_0$, we must take the limit $\Lambda_-^{(0)}\to 0$, not the $s\to 0$ limit. Note that the first factor is necessary to correctly produce this limit, but otherwise it is immaterial as mentioned previously.

The mean-field Helmholtz free energy is related to the grand potential by Eq. (23) with the mean-field densities, Eq. (28). The chemical potentials at zero loop are $\mu_{\pm}^{(0)}=-V_0+\ln(\theta_{\pm}^{(0)}a_{\pm}^3)$, where $V_0\equiv\frac{l_B}{2}\int\frac{d^2\mathbf{q}}{(2\pi)^2}\frac{1}{2q}$, is the bare self-energy (5) for ions that have the same valence. The free energy, again, has a volume (bulk) and a surface contribution of the form $\beta F_0=\beta f_B^{(0)}\mathcal{V}+\beta f_S^{(0)}\mathcal{A}$, with

$$\beta f_B^{(0)} = -\frac{\kappa^2}{l_B}V_0 + \frac{\kappa^2}{l_B}\left[\ln\left(\frac{\kappa^2 a^3}{2l_B}\right)-1\right], \tag{31}$$

$$\beta f_S^{(0)} = -\frac{4(\sqrt{1+s^2}-s)}{l_B\lambda}V_0 + \frac{2}{l_B\lambda}\ln(a_+^3/a_-^3) + \frac{8}{l_B\lambda}\ln\left(\frac{1+\sqrt{1+s^2}}{s}\right) + \frac{4}{l_B\lambda}(\sqrt{1+s^2}-s)\left[\ln\left(\frac{\kappa^2 a^3}{2l_B}\right)-2\right], \tag{32}$$

where $a\equiv(a_+a_-)^{1/2}$. Apart from the self-energy term V_0, Eq. (31) is just the free energy density for an ideal gas with a concentration of $2c_s$. In the limit $\Lambda_-^{(0)}\to 0$, Eq. (32) reduces to the surface free energy density for a system with a charged surface and counterions. Note that the infinite bare self-energy V_0 terms in Eqs. (31) and (32) may be considered higher order terms in l_B since $V_0\sim l_B$, and thus they may be discarded. However, as we will see in Sec. III D, all the infinite bare self-energy terms are canceled, leaving the free energy at one loop perfectly finite.

III. FLUCTUATION EFFECTS

In this section, we investigate in detail fluctuation effects in a highly charged surface immersed in an electrolyte solu-

tion, as outlined in Sec. II A. In the subsequent sections, we first construct the Green's function, which not only is a central quantity underlying our computational technique for evaluating the one-loop correction to free energy, but also has a physical meaning that is fundamental to understanding correlation effects for our system. In particular, we discuss the self-energy of an ion and the interaction potential for two macroions near the charged surface. Both quantities are directly related to the Green's function. In Sec. III B, we solve for the one-loop correction to the electrostatic potential and discuss charge renormalization of the charged surface. In Sec. III C, we discuss ion distributions at one loop. In Sec. III D, we evaluate the grand potential and free energy at one loop explicitly and discuss the surface tension of the charged surface.

A. Construction of the Green's function

The Green's function $G(\mathbf{x},\mathbf{x}')$, which is the inverse of the operator $K(\mathbf{x},\mathbf{x}')$ introduced in Eq. (14), satisfies

$$\{-\nabla_{\mathbf{x}}^2 + \kappa^2 \cosh[\varphi_0(z)]\}G(\mathbf{x},\mathbf{x}') = l_B\delta(\mathbf{x}-\mathbf{x}'). \quad (33)$$

Using the identity $\cosh[\varphi_0(z)]=1+2\,\mathrm{csch}^2\,\kappa(|z|+z_0)$, and Fourier transforming, we may write Eq. (33) as

$$\left[-\frac{\partial^2}{\partial z^2} + 4\alpha^2\kappa^2 + 2\kappa^2\,\mathrm{csch}^2\,\kappa(|z|+z_0)\right]G(z,z';q) = l_B\delta(z-z'), \quad (34)$$

where $4\alpha^2 \equiv 1+q^2/\kappa^2$. To construct the Green's function $G(z,z';q)$, we take, for the moment, a fix $z'>0$, we split space into three distinct regions, and we define in each of the regions

$$G_>(z,z';q) = A(z')h_-(z) \quad \text{for } z>z',$$

$$G_<(z,z';q) = B(z')h_-(z) + C(z')h_+(z), \quad 0<z<z',$$

$$G_-(z,z';q) = D(z')h_-(-z) \quad ,-\infty<z<0,$$

where $h_\pm(z)$ are two independent homogeneous solutions to Eq. (34) given by

$$h_\pm(z) = e^{\pm 2\alpha\kappa z}\left[1 \mp \frac{\coth\,\kappa(z+z_0)}{2\alpha}\right], \quad (35)$$

for $z>0$. To determine the coefficients $A(z')$, $B(z')$, $C(z')$, and $D(z')$, we impose the following boundary conditions on $G(z,z';q)$:

$$G_-(0,z';q) = G_<(0,z';q),$$

$$\partial_z G_-(z,z';q)|_{z=0} = \partial_z G_<(z,z';q)|_{z=0},$$

$$G_<(z,z';q)|_{z=z'} = G_>(z,z';q)|_{z=z'},$$

$$\partial_z G_<(z,z';q)|_{z=z'} = l_B + \partial_z G_>(z,z';q)|_{z=z'}.$$

The first two conditions reinforce that the Green's function $G(z,z';q)$ and its derivative are continuous across $z=0$. The next two conditions reinforce that the Green's function is continuous across $z=z'$, and that its derivative is discontinuous as demanded by the delta-function in Eq. (34). After some algebra, we arrive at

$$G(z,z';q) = \frac{l_B}{2q^2}\sqrt{\kappa^2+q^2}\begin{cases} h_-(-z)h_-(z')[\mathcal{M}(q\lambda)+h_+(0)/h_-(0)] & \text{for } -\infty<z<0, \\ [h_+(z)+\mathcal{M}(q\lambda)h_-(z)]h_-(z') & \text{for } 0<z<z', \\ h_-(z)[h_+(z')+\mathcal{M}(q\lambda)h_-(z')] & \text{for } z>z', \end{cases} \quad (36)$$

where

$$\mathcal{M}(y) \equiv \frac{\sqrt{1+s^2}}{(\sqrt{1+s^2}+\sqrt{s^2+y^2})(1+\sqrt{1+s^2}\sqrt{s^2+y^2}+s^2+y^2)}. \quad (37)$$

The Green's function $G(z,z';q)$ for the case when $z'<0$ can be obtained by simply putting $z'\to -z'$ in Eq. (36), as expected from the symmetry of the system. It can be seen from Eq. (36) that $G(z,z';q)$ is manifestly invariant under the exchange of $z\leftrightarrow z'$, as it should be. We note in passing that if we take the limit $\kappa\to 0$, we recover the Green's function for the case of counterions only for a similar problem, where the counterions are distributed on both sides of the charged surface [44].

An important quantity derived from the Green's function is the self-energy of an ion. It is defined as

$$\beta V_s(z) = \int \frac{d^2\mathbf{q}}{(2\pi)^2}\left[G(z,z;q) - \frac{l_B}{2q}\right]. \quad (38)$$

The physical meaning of the self-energy is that it represents the energy an ion gained when the ion is brought from vacuum to the vicinity of the charged plate. There are two contributions to the self-energy: the Debye-Huckel contribution

$$G_{\mathrm{DH}}(0) \equiv \frac{l_B}{2}\int \frac{d^2\mathbf{q}}{(2\pi)^2}\left(\frac{1}{\sqrt{\kappa^2+q^2}} - \frac{1}{q}\right) = -\frac{l_B\kappa}{4\pi} \quad (39)$$

and a contribution due to the presence of the plate

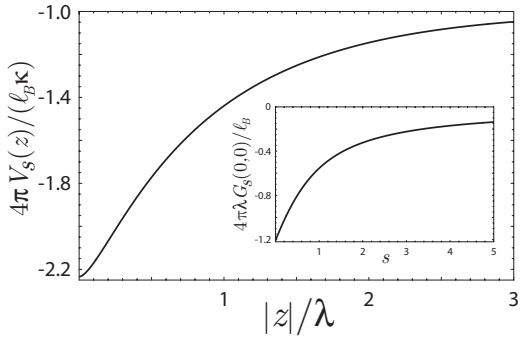

FIG. 2. The self-energy of an ion near a charged surface immersed in an electrolyte solution, $\beta V_s(z)$ defined by Eq. (38), as a function of z for $s \equiv \kappa\lambda = 0.6$. The physical meaning of $\beta V_s(z)$ is the energy that it takes to bring the ion from vacuum to a distance z from the plate. (Inset) $G_s(0,0)$ vs s, as given by Eq. (43). The physical interpretation of $G_s(0,0)$ is the correlation energy arising from the charged surface.

$$G_s(z,z) \equiv \int \frac{d^2\mathbf{q}}{(2\pi)^2} G_s(z,z;q), \tag{40}$$

where

$$G_s(z,z;q) \equiv \frac{l_B}{2q^2}\frac{\kappa^2}{\sqrt{\kappa^2+q^2}}\{-\operatorname{csch}^2\kappa(|z|+z_0) + \mathcal{M}(q\lambda)e^{-4\alpha\kappa|z|}[2\alpha+\coth\kappa(|z|+z_0)]^2\}. \tag{41}$$

Although an analytic but complicated expression for $\beta V_s(z)$ can be obtained (see Appendix A), it is more instructive to give the asymptotics of $\beta V_s(z)$ (see also Fig. 2). For large $|z|\to\infty$, $G_s(z,z)$ decays exponentially to zero, and $\beta V_s(z) = -l_B\kappa/(4\pi) + O(e^{-2\kappa|z|})$, when s is finite. Therefore, as expected, the self-energy of an ion far away from the charged surface is given by the self-energy in the bulk, which is just the self-energy for an ion immersed in an electrolyte solution. On the other hand, in the limit $s\to 0$ (GC regime), we find $\beta V_s(z) \simeq -l_B/(6\pi|z|) + O[s, 1/z^2]$, which decays algebraically for large z. For small z, we find

$$\beta V_s(z) = -\frac{l_B\kappa}{4\pi} + G_s(0,0) + O(z^2). \tag{42}$$

Here, $G_s(0,0)$ may be interpreted as the energy to bring an ion initially at infinity to the charged surface at $z=0$; it is given by a simple formula

$$G_s(0,0) = -\frac{l_B}{2\pi\lambda\sqrt{s^2-3}}\tanh^{-1}\left(\frac{\sqrt{s^2-3}}{2s+\sqrt{1+s^2}}\right). \tag{43}$$

Note that $G_s(0,0) < 0$, which means that an ion, regardless of its sign, gains energy by being closer to the charged surface. For $s \ll 1$, $G_s(0,0) \simeq -(l_B/\lambda)[1/(6\sqrt{3}) - s/(4\pi)]$, while for $s \gg 1$, $G_s(0,0) \simeq -l_B\kappa \tanh^{-1}(1/3)/(2\pi s^2)$, as shown in the inset of Fig. 2. Note that in both cases, $G_s(0,0)$ vanishes in the limit $\lambda\to\infty$ or vanishing surface charge density on the surface, as it should be.

It is important to point out that the shape of $\beta V_s(z)$ at small z, as shown in Fig. 2, differs qualitatively from that of Ref. [26], where the the authors obtained the self-energy of an ion for a system of counterions near an impenetrable charged wall. In particular, our $\beta V_s(z)$ does not exhibit a minimum at a little distance away from the surface as does the one obtained in Ref. [26]. The origin of this difference arises from the fact that the charged surface in our system is assumed to be permeable to the ions and is not an impenetrable hard wall. In the latter case, since the ions are only distributed on one side of the surface, an ion of either sign experiences a repulsion from the surface due to an increase of the effective dielectric constant on one side containing the salt solution [45]. This effect, however, does not occur in our system, since there are charges on both sides. Therefore, correlation effects for these two systems can be subtly different, even though, at the mean-field level, the two systems are characterized by the same expressions for electrostatic potential and ion distributions. Note, however, that the Gouy-Chapman lengths for the two systems are different by a factor of 2 due to different boundary conditions. As we will see in Sec. III C, the counterion distributions are indeed qualitatively different near the surface for the two systems.

The Green's function $G(\mathbf{x},\mathbf{x}')$ can also be interpreted as the interaction potential between two test charges located at $\mathbf{x}$ and $\mathbf{x}'$ in the presence of fluctuating ions in the bulk as well as those near the charged surface. It plays the same role as the screened Coulomb potential in the Debye-Huckel theory for a homogeneous electrolyte solution. Therefore, $G(\mathbf{x},\mathbf{x}')$ is an important quantity to access the physical behavior of charged colloidal particles near charged surfaces, a subject that is being actively explored experimentally [20,21]. For simplicity, let us consider two test charges of the same sign located at the same distance z away from the surface and they are separated by a separated by a distance r from each other. The interaction is given by

$$G(z,r) \equiv \int_0^\infty \frac{dq\, q}{2\pi} G(z,z;q) J_0(qr), \tag{44}$$

where $J_0(qr)$ is the Bessel function of the first kind of order zero. Unfortunately, Eq. (44) cannot be integrated in closed form, but it can be numerically integrated without any difficulty.

In Fig. 3, we plot the interaction as a function of the separation between two test charges for different values of z/λ and s. When the two charged particles are far away from the charged surface ($z \gg \lambda$), the interaction reduces to the screened Coulomb potential

$$G(z,r) = \frac{l_B e^{-\kappa r}}{4\pi r} + O[e^{-2\kappa z}], \tag{45}$$

as expected. On the other hand, when the test charges are close to the charged surface ($z \ll \lambda$), the repulsion between them is substantially suppressed (although there is no attraction), as can be seen from Fig. 3. Indeed, in the $z\to 0$ limit, the interaction can be shown to be

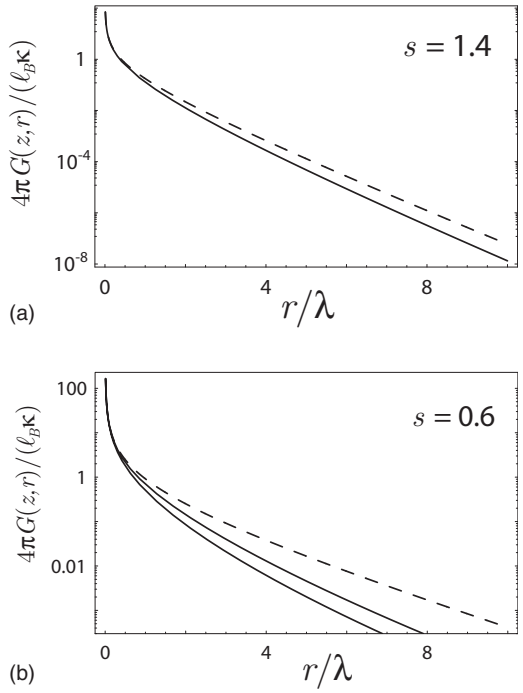

FIG. 3. A linear-log plot of the Green's function $G(z,r)$ vs r for $z/\lambda=\infty$ and 0.01 and $s=1.4$ (a) and for $z/\lambda=\infty$, 1, and 0.01 and $s=0.6$ (b). $G(z,r)$ can be interpreted as the electrostatic interaction potential between two test charges at a distance z away from the surface and separated by r. The dashed lines represent the screened Coulomb potential. When the charges are in close vicinity of the charge plate, their interaction is drastically reduced. In the GC regime ($s \ll 1$), the interaction goes as $G(z,r) \sim r^{-5}$.

$$G(0,r) = \frac{l_B}{4\pi\lambda}\int_0^\infty \frac{dy\, yJ_0(yr/\lambda)(\sqrt{1+s^2}+\sqrt{s^2+y^2})}{1+\sqrt{1+s^2}\sqrt{s^2+y^2}+s^2+y^2}. \tag{46}$$

At large r, $G(0,r)$ has the following interesting asymptotic expansions: when $s \gg 1$ (low surface charge), we find

$$G(0,r) \simeq \frac{l_B}{4\pi\sqrt{1+s^2}}\frac{e^{-\kappa r}}{r}. \tag{47}$$

Thus, the two charges of the same sign with a magnitude q would interact as if they had a reduced charge of $q^* \simeq q/(1+s^2)^{1/4} < q$. More importantly, we find from Eq. (46) that when $s \ll 1$ (high surface charge),

$$G(0,r) \simeq \frac{9l_B\lambda^4}{4\pi r^5} + O(s). \tag{48}$$

Thus, their repulsion varies inversely with the separation raised to the fifth power. We note that the van der Waals attraction between two charged colloids varies as $-1/r^3$, which has a longer range than the electrostatic repulsion in this case. This observation suggests an overall qualitatively different behavior for a system of charged colloids near a highly charged surface than that in the bulk.

B. One-loop correction to the electrostatic potential and charge renormalization

In this section, we discuss the one-loop correction to the electrostatic potential; we have already presented its formal expression in Eq. (20). Instead of dealing with an integral equation, we can gain more physical insights by converting Eq. (20) into a differential equation using the property of the Green's function, Eq. (33); we find that $\langle[\imath\Delta\psi(\mathbf{x})]\rangle_1$ satisfies

$$\{-\partial_z^2 + \kappa^2\cosh[\varphi_0(z)]\}\langle[\imath\Delta\psi(z)]\rangle_1 = \frac{1}{2}G(z,z)H(z) - F(z), \tag{49}$$

where we have used the fact that the problem depends only on z. Note that Eq. (49) can also be derived directly from the exact relation Eq. (10). The functions $F(z)$ and $H(z)$, defined by Eqs. (16) and (17), respectively, can be written as $F(z) = \kappa^2[\omega_+ \sinh\varphi_0(z) + \omega_- \cosh\varphi_0(z)]$ and $H(z) = \kappa^2 \sinh\varphi_0(z)$, where we have defined

$$\omega_\pm \equiv \frac{1}{2}(\delta\Lambda_+/\Lambda_+^{(0)} \pm \delta\Lambda_-/\Lambda_-^{(0)}). \tag{50}$$

Since Eq. (49) is a second-order ordinary differential equation, we must specify two boundary conditions. The obvious boundary condition is $\langle[\imath\Delta\psi(\mathbf{x})]\rangle_1 \to 0$ as $|z| \to \infty$. This immediately implies that $\omega_-=0$, since $\langle[\imath\Delta\psi(\mathbf{x})]\rangle_1 = -\omega_-$ is one of the particular solutions to Eq. (49), or, equivalently, since the electrostatic potential is defined only up to a constant, we can safely set $\omega_-=0$ without sacrificing any physical content. Splitting $G(\mathbf{x},\mathbf{x})$ as a sum of three contributions $G(\mathbf{x},\mathbf{x}) = 2V_0 - l_B\kappa/(4\pi) + G_s(z,z)$, and setting

$$\omega_+ = V_0 - \frac{l_B\kappa}{8\pi}, \tag{51}$$

we can see that the right-hand side of Eq. (49) becomes simply

$$\frac{1}{2}G(z,z)H(z) - F(z) = \frac{\kappa^2}{2}G_s(z,z)\sinh\varphi_0(z). \tag{52}$$

It is important to point out that choosing ω_+ according to Eq. (51) is crucial for rendering the one-loop potential $\langle[\imath\Delta\psi(\mathbf{x})]\rangle_1$, finite since the right-hand side of Eq. (49) as now given by Eq. (52) does not contain the (infinite) bare self-energy V_0. Moreover, as we show in Sec. III D, Eq. (51) is necessary for canceling out all the divergences in the one-loop free energies. Note also that the finite part of ω_+, $-l_B\kappa/(8\pi)$, is determined by demanding that the one-loop correction to the chemical potential must coincide with that of the Debye-Huckel result; see Eq. (69) below. Indeed, as we show in Sec. III D, it is required to correctly produce thermodynamic quantities in the bulk at the one-loop level, e.g., the pressure and the free energy density.

The second boundary condition can be obtained from the charge neutrality condition (1). Using the ion distributions at one loop, Eq. (21) and the fact that the mean-field densities

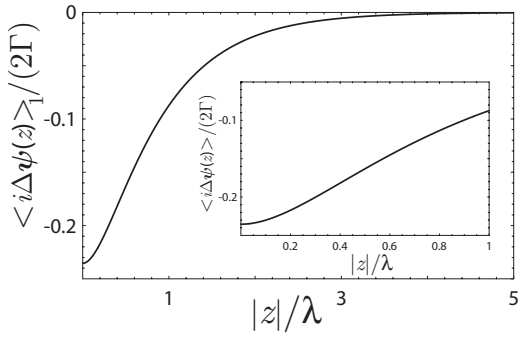

FIG. 4. The one-loop correction to the potential $\langle \imath\Delta\psi(z)\rangle_1/(2\Gamma)$ as given by Eq. (54) for $s=1.4$, where $\Gamma \equiv l_B\kappa/(32\pi)$. Note that the derivative of $\langle \imath\Delta\psi(z)\rangle_1$ at $z=0$ is zero (inset), as required by charge neutrality.

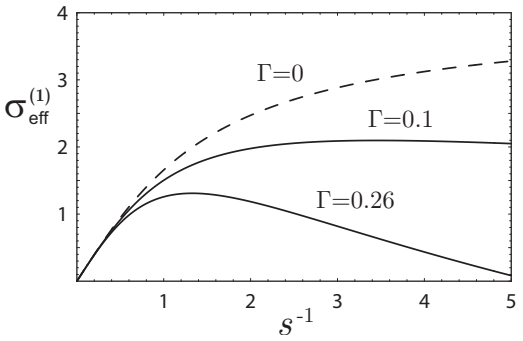

FIG. 5. The renormalized surface charge density $\sigma_{\rm eff}^{(1)}(s)$ versus $1/s$ for $\Gamma \equiv l_B\kappa/(32\pi)=0.1$ and 0.26. Note that $1/s=l_Bn_0/(4Z\kappa)$ is proportional to the bare surface density n_0.

already satisfy the charged neutrality condition [see Eq. (29)], we find that charge neutrality condition at one loop states that

$$\int d^3\mathbf{x}\langle \imath\Delta\psi(\mathbf{x})\rangle_1 \cosh[\varphi_0(\mathbf{x})] - \frac{1}{2}\int d^3\mathbf{x}G_s(\mathbf{x},\mathbf{x})\sinh[\varphi_0(\mathbf{x})] = 0. \tag{53}$$

Using Eq. (49) in conjunction with Eq. (52), the above condition can be transformed into $\int_{-\infty}^{\infty} dz\partial_z^2\langle \imath\Delta\psi(z)\rangle_1=0$, which implies that $\partial_z \langle \imath\Delta\psi(z)\rangle|_{z=0}=0$, since the symmetry of the problem dictates that $\langle \imath\Delta\psi(z)\rangle_1$ is symmetric with respect to $z\leftrightarrow -z$. It is straightforward to find all the particular solutions to Eq. (49) (see Appendix B); our final result for the one-loop correction to the electrostatic potential can be expressed as

$$\langle \imath\Delta\psi(z)\rangle_1 = \frac{l_B\kappa}{16\pi}[\mathcal{A}(s)-\mathcal{F}(z)]\mathrm{csch}\ \kappa(|z|+z_0), \tag{54}$$

where $\mathcal{F}(z)$ is defined and evaluated in Eq. (B6), and $\mathcal{A}(s)$ is defined in Eq. (B5) and it can be explicitly evaluated to give

$$\mathcal{A}(s) = -\frac{2}{\sqrt{1+s^2}\sqrt{s^2-3}}\tanh^{-1}\left(\frac{\sqrt{s^2-3}}{2s+\sqrt{1+s^2}}\right) - \ln\left[\frac{\sqrt{1+s^2}(\sqrt{1+s^2}+s)}{2s^2}\right]. \tag{55}$$

It is straightforward to verify explicitly that Eq. (54) satisfies Eq. (49) along with all the boundary conditions, and in particular, the charge neutrality condition (53). Note also that Eq. (54) can be derived directly from performing the integrals in Eq. (20).

In Fig. 4, we plot $\langle \imath\Delta\psi(z)\rangle_1$ as a function of z. Note first that $\langle \imath\Delta\psi(z)\rangle_1$ is negative for all values of s and z, so that it reduces the mean-field potential (see also Fig. 6). Therefore, correlation enhances the screening of a charged surface. For small z, we find $\langle \imath\Delta\psi(z)\rangle_1 \simeq l_B\mathcal{A}(s)/(16\pi\lambda)+O(z^2)$, the derivative of which is clearly zero at $z=0$, as required by charge neutrality (see inset of Fig. 4). For large z, we have two cases to consider. First, in the limit $s\to 0$, we find $\langle \imath\Delta\psi(z)\rangle_1 \simeq 2\ln(\kappa z)$. Second, for finite s, we find, for large z, that

$$\langle \imath\Delta\psi(z)\rangle_1 \simeq \frac{l_B\kappa}{8\pi}(\sqrt{1+s^2}-s)\mathcal{A}(s)e^{-\kappa|z|}, \tag{56}$$

from which we identify, in analogy to Eq. (27), a renormalized surface charge density at one loop to be

$$\sigma_{\rm eff}^{(1)}(s) \equiv 4s\left(\sqrt{1+\frac{1}{s^2}}-1\right)\left[1+\frac{l_B\kappa}{32\pi}\mathcal{A}(s)\right]. \tag{57}$$

For finite s, the renormalized charge at one loop is always lower than the renormalized charge given by the mean-field theory, Eq. (27), as can be seen in Fig. 5. For low surface charge $s\gg 1$, we find that $\sigma_{\rm eff}^{(1)}(s)=2/s+O(s^{-2})$. Thus, for sufficiently low surface charge, there is no charge renormalization even when correlation is included. On the other hand, for highly charged surfaces, $s\ll 1$, $\sigma_{\rm eff}^{(1)}(s)\simeq 4(1+2\Gamma\ln s)$, which can become negative for sufficiently large $\Gamma \equiv l_B\kappa/(32\pi)$. It is clear from Eq. (57) that there is a critical $\Gamma_c(s)=-1/\mathcal{A}(s)$, above which the effective charge becomes negative. This phenomenon is called charge inversion, which has been discussed intensively in the literature [7]. For $s\gg 1$, we find that $\Gamma_c(s)\sim s^2$, while $s\ll 1$, $\Gamma_c(s)\sim[\ln(1/s)]^{-1}$. For an order of magnitude estimate, taking $n_0\sim 1/100$ Å^2, $\kappa^{-1}\sim 100$ Å, and divalent counterions at room temperature, we find $\sigma_{\rm eff}^{(1)}\sim 2.2$, which is about 40% more of a reduction to the actual surface charge than that predicted by the mean-field theory ($\sigma_{\rm eff}^{(0)}\sim 3.9$).

We note in passing that our exact expression for the effective charge (57) differs from that of Ref. [24], although qualitatively they exhibit the same trend, with one notable difference: the authors of Ref. [24] found that as $s\to\infty$, the effective charge is renormalized by a finite amount, whereas we find that it is not renormalized. The origin of this difference may be attributed to (i) the authors of Ref. [24] considered a system of ions (positive and negative) in contact with two charged hard walls, whereas the present problem is formulated for a permeable charged surface and (ii) the authors of Ref. [24] obtained the expression for the effective charge from the asymptotic behavior of the pressure in the limit of

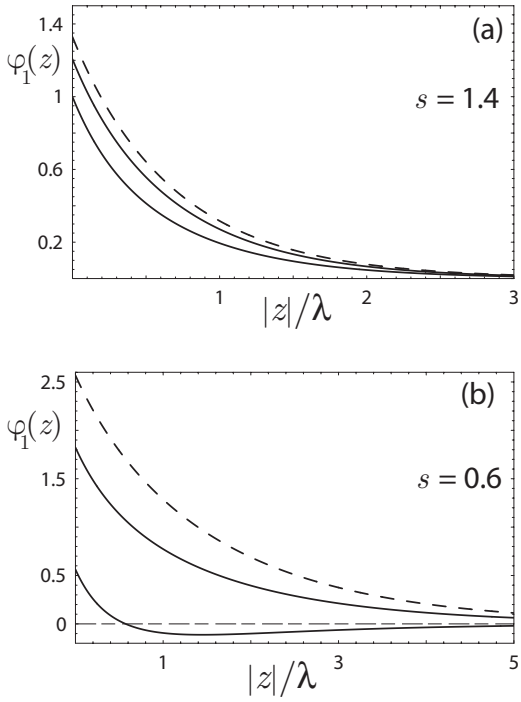

FIG. 6. The electrostatic potential to one-loop order $\varphi_1(z) \equiv \varphi_0(z) + \langle \imath \Delta \psi(z) \rangle_1$ for $s=1.4$ (a) and $s=0.6$ (b). From the top curves $\Gamma \equiv l_B \kappa/(32\pi)=0$, 0.26 , and 0.7. Note that correlation effects are more prominent for highly charged surface charge $s<1$, as expected. Furthermore, for sufficiently high Γ, $\varphi_1(z)$ becomes negative, indicating charge inversion.

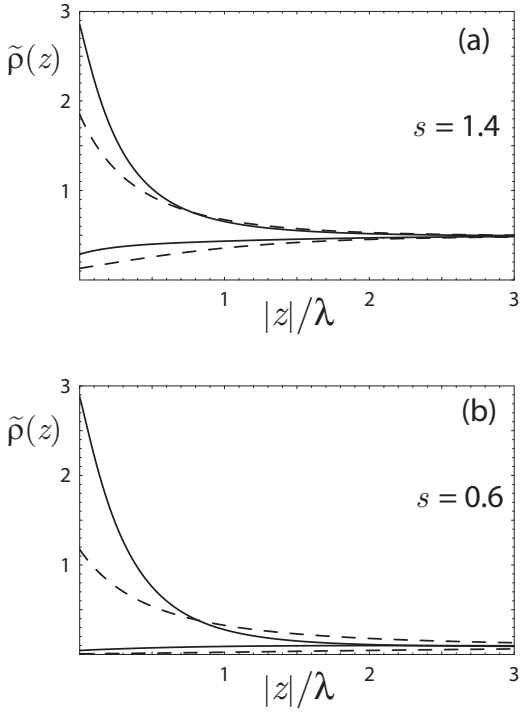

FIG. 7. The normalized ion distributions $[\tilde{\rho}_{\pm}(z) \equiv (l_B \lambda^2/2) \times \langle \hat{\rho}_{\pm}(z) \rangle_1]$ to one-loop order for $s=1.4$ (a) and $s=0.6$ (b). The dashed lines represent mean-field ion profiles. In (a) and (b), the top dashed curves represent counterion profiles and the bottom dashed curves represent coion profiles. The solid curves present one-loop ion distributions with $\Gamma \equiv l_B \kappa/(32\pi)=0.7$.

large separations between the two hard walls, whereas Eq. (57) was obtained from the asymptotic behavior of the electrostatic potential, as is done traditionally, at the one-loop level. Thus, there may be a difference in the definitions of the effective charges. We also note that the Wigner crystal approach predicts that charge inversion occurs when $\Gamma_c(s) \sim s^{-2}$ [14], which is different from above.

As specific examples, in Fig. 6, we plot the electrostatic potential at the one-loop level: $\varphi_1(z) \equiv \varphi_0(z) + \langle \imath \Delta \psi(z) \rangle_1$. As can be seen, it is generally smaller than the mean-field potential, and for a fixed Γ, this reduction is more dramatic in the GC regime ($s<1$) than in the DH regime ($s>1$). For sufficiently large Γ, the electrostatic potential becomes negative at intermediate z, which is the result of charge inversion. The electrostatic potential at the surface $\varphi_1(0)$ is related (in some cases) to the zeta potential which can be extracted from electrokinetic measurements [3], and $\varphi_1(0)=2\ln[(1+\sqrt{1+s^2})/s]+[l_B/(16\pi\lambda)][\mathcal{A}(s)-\mathcal{F}(0)]$. For small s, we find $\varphi_1(0)=-2\ln(s/2)-l_B/(16\sqrt{3}\lambda)+O(s)$, while for large s, we find $\varphi_1(0)=2/s-l_B[\ln 4-1/2]/(16\pi\lambda s^2)+O(1/s^3)$. We end this subsection by emphasizing that even though our one-loop calculation predicts charge inversion, higher order terms in the loop expansion may become prominent before the effective charge changes sign.

C. Ion distributions at one loop

Using Eq. (21) and the results from previous sections, we can express the one-loop ion distributions as

$$\langle \hat{\rho}_{\pm}(z) \rangle_1 = \frac{\kappa^2 e^{\pm \varphi_0(z)}}{2 l_B} \left[1 \pm \langle \imath \Delta \psi(z) \rangle_1 - \frac{1}{2} G_s(z,z) \right]. \quad (58)$$

In Figs. 7 and 8, we plot the ion distributions for different values of s and Γ. As can be seen, there are, in general, more ions of both signs near the charged surface (though the effect is more drastic for counterions than for coions) than predicted by the mean-field theory. This is because, as we have seen in Sec. III A, correlation enhances the energy gained for an ion, regardless of its sign, when it is closer to the surface. In particular, there is an increase in the counterion density

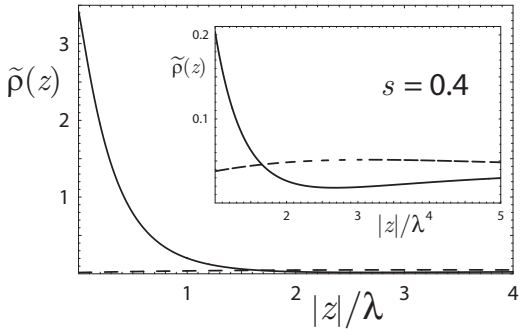

FIG. 8. The normalized ion distributions to one-loop order for $s=0.4$ and $\Gamma=0.7$. The solid (dashed) curve represents the counterion (coion) profile. The inset shows the formation of a secondary coion layer.

with respect to the mean-field counterion density, at length scale $z<z^*$, where z^* is determined by $\langle \imath\Delta\psi(z^*)\rangle_1 - G_s(z^*,z^*)/2=0$, while for $z>z^*$ the counterion density is lower than the mean-field counterion density. This is not surprising since charges are conserved. Note that z^* is always less than the Gouy-Chapman length λ and z^* roughly decreases with increasing s.

The counterion density at the surface can be substantially larger than that predicted by the mean-field theory; the deviation is given by $\Delta\rho_+(0)/\rho_+^{(0)}(0)=\langle \imath\Delta\psi(0)\rangle_1 - G_s(0,0)/2$, which scales as $\Delta\rho_+(0)/\rho_+^{(0)}(0)\sim\Gamma/s$ for $s\ll 1$, and $\Delta\rho_+(0)/\rho_+^{(0)}(0)\sim\Gamma/s^2$ for $s\gg 1$. Thus, deviations from mean-field behaviors are more prominent in the GC regime, $s<1$, than in the DH regime, $s>1$, as expected. For sufficiently large Γ, the counterion density at intermediate z starts to develop a minimum which has a lower value than density in bulk, while the coion density starts to develop a maximum, which in some cases, depending on Γ, has a value higher than the counterion density. Thus, at some large Γ, a second layer of coions forms as can be seen in the inset of Fig. 8. This effect has been observed in a recent simulation [34], and it exemplifies the dramatic consequences of correlation effects in the system. For large z, we find

$$\langle \hat{\rho}_+(z)\rangle_1 \simeq \frac{\kappa^2}{2l_B}[1+\sigma_{\text{eff}}^{(1)}(s)e^{-\kappa|z|}]. \tag{59}$$

Thus, the formation of the second layer of coions and the electrostatic potential being negative are all manifestations of charge inversion. We remark in passing that the potential of mean force, which is related to the ion profiles by $\beta W_\pm(z) \equiv \ln[(2l_B/\kappa^2)\langle\hat{\rho}_\pm(z)\rangle_1] = \mp\varphi_1(z)+\frac{1}{2}G_s(z,z)$, can be probed experimentally by an atomic force microscope technique [13], thus providing a connection of correlation effects studied theoretically here to experiments.

It might be important to point out that the behavior of the counterion density differs qualitatively from that of Ref. [26], where the counterion density at the surface coincides with the mean-field counterion density to ensure that the contact value theorem is obeyed. The contact value theorem states that the pressure at the surface must equal to the pressure in the bulk [40]. Physically, it means that if the charged wall is in equilibrium with the counterion gas, it must also be in mechanical equilibrium with the counterion gas or else the charged wall would move. Note that our one-loop solution violates the contact value theorem. The simple reason underlying this violation arises from that our problem is formulated for permeable surfaces and the contact value theorem needs not hold. This is because our system is symmetric with respect to both sides of the surface: the electrostatic contribution to the pressure across the surface includes a contribution from fluctuations in the ion distributions on both sides of the plate.

It is clear that for very large Γ, the counterion density becomes negative. We take this to be the upper bound of $\Gamma_u(s)$ at which our one-loop solution is no longer valid. For example, we find that for $s\sim 1$, $\Gamma_u\sim 6$. Note that in order to get exactly when the one-loop correction breakdown, we must go to a higher loop or compare our results with computer simulations. We defer a discussion on the validity of our one-loop correction to Sec. IV.

D. Fluctuation contributions to the free energies

In this section, we evaluate the one-loop correction to the grand potential and to the free energy. Using Eq. (22), the grand potential can be written as

$$\beta\Omega_1[\phi] = \beta\Omega_0[\phi] + \frac{1}{2}\ln\det\hat{\mathbf{K}} - \frac{1}{2}\ln\det[-\nabla_{\mathbf{x}}^2/l_B] - \frac{\kappa^2}{l_B}\left(V_0 - \frac{l_B\kappa}{8\pi}\right)\int d^3\mathbf{x}\cosh\varphi_0(z), \tag{60}$$

where we have used the fact that $\omega_-=0$ and $\omega_+=V_0 - l_B\kappa/(8\pi)$, as determined in Sec. III B. The fundamental quantity to evaluate is the functional determinant

$$\beta\Delta\Omega \equiv \frac{1}{2}\ln\det\hat{\mathbf{K}} - \frac{1}{2}\ln\det[-\nabla_{\mathbf{x}}^2/l_B], \tag{61}$$

where $\hat{\mathbf{K}}\equiv[-\nabla_{\mathbf{x}}^2+\kappa^2\cosh\varphi_0(\mathbf{x})]/l_B$, defined in Eq. (14). In principle, in order to evaluate Eq. (61), we have to find the eigenvalues and eigenfunctions to the operator $\hat{\mathbf{K}}$ with appropriate boundary conditions and reexpress $\nabla_{\mathbf{x}}^2$ in terms of those eigenvalues. Equation (61), then, corresponds to the difference between the sum of the logarithm of the eigenvalues for $\hat{\mathbf{K}}$ and the sum of the logarithm of the eigenvalues for $-\nabla_{\mathbf{x}}^2$. For spatially uniform systems, e.g., the Debye-Huckel theory, this procedure can be easily carried out via Fourier transform. However, for spatially nonuniform systems, which is the case for our system, this procedure seems laborious at best and it has only been attempted in Refs. [24,25].

Here, we adopt a trick which has been employed previously to study fluctuation effect in counterion-only systems [27]; it is based on the identity $\delta\ln\det\hat{\mathbf{X}}=\mathrm{Tr}\,\hat{\mathbf{X}}^{-1}\delta\hat{\mathbf{X}}$, for any operator $\hat{\mathbf{X}}$. As shown below, this identity allows us to evaluate exactly the functional determinant (61) in a straightforward manner, which does not involve an *ad hoc* subtraction scheme to cancel the infinite bare energy. Thus, differentiating Eq. (61) with respect to l_B and using the identity above, we find

$$\frac{\partial\beta\Delta\Omega}{\partial l_B} = \frac{1}{2l_B}\int d^3\mathbf{x}G(\mathbf{x},\mathbf{x})\frac{\partial}{\partial l_B}[\kappa^2\cosh\varphi_0(z)], \tag{62}$$

where we have made use of the fact that the inverse of $\hat{\mathbf{K}}$ in position space is the Green's function $G(\mathbf{x},\mathbf{x}')$ and that the trace in position space corresponds to setting $\mathbf{x}=\mathbf{x}'$ and integrating over space. Writing $G(\mathbf{x},\mathbf{x})$ as a sum of three contributions $G(\mathbf{x},\mathbf{x})=2V_0-l_B\kappa/(4\pi)+G_s(z,z)$, we see that the first term in Eq. (62), which represents the bare self-energy term, precisely cancels the bare self-energy term in Eq. (60). Therefore, the final result for $\beta\Omega_1[\phi]$ is perfectly finite, as it should be.

The second term gives the Debye-Huckel contribution

$$\frac{\partial \beta \Delta \Omega_{\mathrm{DH}}}{\partial l_B} \equiv -\frac{\kappa}{8\pi} \int d^3\mathbf{x} \frac{\partial}{\partial l_B} [\kappa^2 \cosh \varphi_0(z)], \tag{63}$$

which contains a volume contribution and a surface contribution. It is straightforward to show that the volume contribution is simply the standard Debye-Huckel result for a homogeneous electrolyte $\beta \Delta F_{\mathrm{DH}}/\mathcal{V} = -\kappa^3/(12\pi)$ [46]. The surface contribution can be written as

$$\left(\frac{\partial \beta \Delta \Omega_{\mathrm{DH}}}{\partial l_B} \right)_S = -\frac{\kappa}{2\pi} \frac{\partial}{\partial l_B} \left(\frac{\sqrt{1+s^2}-s}{\lambda} \right) \cdot \mathcal{A},$$

which can be integrated back with respect to l_B in a straightforward manner by noting that $\kappa \sim \sqrt{l_B}$, $\lambda \sim 1/l_B$, and $s \sim 1/\sqrt{l_B}$. Therefore, we obtain

$$\beta \Delta \Omega_{\mathrm{DH}} = -\frac{\kappa^3 \mathcal{V}}{12\pi} - \frac{s\mathcal{A}}{12\pi\lambda^2} [2(2-s^2)\sqrt{1+s^2} - 3s]. \tag{64}$$

The third term in Eq. (62) arising from the charged plate contains only a surface contribution

$$\frac{1}{\mathcal{A}} \frac{\partial \beta \Delta \Omega_S}{\partial l_B} \equiv \frac{1}{2l_B} \int_{-\infty}^{\infty} dz\, G_s(z,z) \frac{\partial}{\partial l_B} [\kappa^2 \cosh \varphi_0(z)]. \tag{65}$$

In Appendix C, we present the detail of evaluating $\beta \Delta \Omega_S$. The final result for $\beta \Delta \Omega$, defined in Eq. (62), is

$$\beta \Delta \Omega = \beta \Delta \Omega_{\mathrm{DH}} + \beta \Delta \Omega_S = -\frac{\kappa^3}{12\pi} \mathcal{V} - \frac{\mathcal{K}(s)}{8\pi\lambda^2} \mathcal{A}, \tag{66}$$

where

$$\mathcal{K}(s) \equiv \sqrt{(1+s^2)(s^2-3)} \tanh^{-1} \left(\frac{\sqrt{s^2-3}}{2s+\sqrt{1+s^2}} \right) + 2s(\sqrt{1+s^2}-s) - s^2 \ln \left(\frac{s}{\sqrt{1+s^2}} \right) - \frac{1-s^2}{2} \ln \left(1 + \frac{s}{\sqrt{1+s^2}} \right). \tag{67}$$

In Eq. (66), we have discarded the bare self-energy term, since, as mentioned above, it cancels the bare self-energy term in Eq. (60). Note that $\beta \Delta \Omega < 0$, as can be seen from a plot of $\mathcal{K}(s)$ depicted in Fig. 9. Therefore, fluctuations have an overall effect of lowering the free energy, as it should be. For $s \ll 1$, $\mathcal{K}(s) = \pi/\sqrt{3} \approx 1.8$, which agrees with the counterion-only case [44], and for large $s \gg 1$, we find $\mathcal{K}(s) = 2$. Note that in both cases the numerical values of $\mathcal{K}(s)$ do not differ significantly; $\mathcal{K}(s) \simeq 2$; therefore, for all practical purposes, the surface contribution to $\Delta\Omega$ is $\Delta\Omega/\mathcal{A} \simeq -1/(4\pi\lambda^2)$.

The results above may be understood from the following scaling arguments: the fluctuation contribution to the surface free energy, $\Delta\Omega/\mathcal{A}$, may be estimated by multiplying the correlation energy to the total charge density near the charged surface and a length over which the ions are confined: $G_s(0,0)(\kappa^2/l_B)(1+2/s^2)z_0$. For $s \gg 1$, $G_s(0,0) \sim -l_B\kappa/s^2$ and $z_0 \sim \kappa^{-1}$, so that $\Delta\Omega/\mathcal{A} \sim -1/\lambda^2$. On the other hand, for $s \ll 1$, $G_s(0,0) \sim -l_B/\lambda$ and $z_0 \sim \lambda$, and therefore, $\Delta\Omega/\mathcal{A} \sim -1/\lambda^2$, consistent with the results above. Note that, in both cases, $\Delta\Omega/\mathcal{A}$ vanishes as $\lambda \to \infty$ or $n_0 \to 0$, as expected.

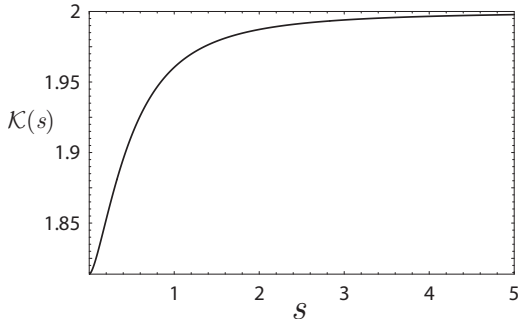

FIG. 9. $\mathcal{K}(s)$, defined in Eq. (67), as a function of s. For small s (highly charged), $\mathcal{K}(s) \simeq \pi/\sqrt{3} = 1.814$, while for large s (low charge), $\mathcal{K}(s) \simeq 2$.

We are now in a position to obtain explicit expressions for the grand potential and the Helmholtz free energy for our system, and more importantly, to extract the surface tension. The grand potential can be expressed as $\beta\Omega_1[\phi] = -p_1\mathcal{V} + \gamma_1(s)\mathcal{A}$. The bulk pressure at one loop p_1 has three contributions: a mean-field contribution $p_0 = \kappa^2/l_B = 2c_s$, a contribution coming from the last term in Eq. (60) and a contribution coming from the functional determinant (64). Therefore, $p_1 = 2c_s - \kappa^3/(8\pi) + \kappa^3/(12\pi) = 2c_s - \kappa^3/(24\pi)$, which is precisely the pressure for a homogeneous electrolyte [46]. Similarly, the surface tension to one loop is

$$\gamma_1(s) = \gamma_0(s) + \frac{s}{2\pi\lambda^2}(\sqrt{1+s^2}-s) - \frac{\mathcal{K}(s)}{8\pi\lambda^2}. \tag{68}$$

As can be seen in Fig. 10, the surface tension is substantially lowered by fluctuation effects. Indeed, at sufficiently high couplings, it becomes negative. Thus, charge fluctuations may drive the system to instability.

The Helmholtz free energy at the one-loop level is related to the grand-canonical potential by Eq. (23) with one-loop ion distributions, (58). The chemical potentials to one loop is now given by

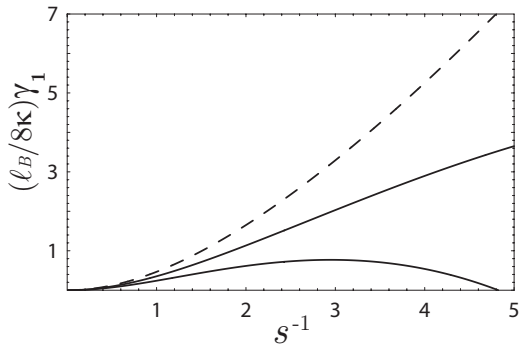

FIG. 10. The electrostatic contribution to the surface tension at one loop vs $1/s$ for (from top to bottom) $\Gamma = 0.2$ and 0.5. The dashed line represents the mean-field surface tension. Note that correlation effects drastically lower the surface tension.

$$\mu_{\pm}^{(1)} = -\frac{l_B\kappa}{8\pi} + \ln\left(\frac{\Lambda_{\pm}^{(0)}a_{\pm}^3}{l_B}\right), \tag{69}$$

where we have used the fact that $\delta\Lambda_{\pm}/\Lambda_{\pm}^{(0)} = V_0 - l_B\kappa/(8\pi)$, as given by Eq. (51). It is important to point out that, in contrast to the chemical potentials at zero loop, $\mu_{\pm}^{(1)}$ is perfectly finite. We find that the bulk contribution to the free energy is

$$\beta f_B^{(1)} = -p_1 - \frac{\kappa^3}{8\pi} + \frac{\kappa^2}{l_B}\ln\left(\frac{\kappa^2 a^3}{2l_B}\right) = 2c_s[\ln(c_s a^3) - 1] - \frac{\kappa^3}{12\pi}, \tag{70}$$

which is precisely the Debye-Huckel free energy, and that the surface contribution is given by

$$\begin{aligned}\beta f_S^{(1)} = {} & \frac{2}{l_B\lambda}\ln(a_+^3/a_-^3) + \frac{8}{l_B\lambda}\ln\left(\frac{1+\sqrt{1+s^2}}{s}\right) \\ & + \frac{4}{l_B\lambda}(\sqrt{1+s^2} - s)\left[\ln\left(\frac{\kappa^2 a^3}{2l_B}\right) - 2\right] \\ & + \frac{1}{8\pi\lambda^2}\left[\frac{s^2\mathcal{J}_A(s)}{1+s^2}\ln\left(\frac{\kappa^2 a^3}{2l_B}\right) - \mathcal{K}(s)\right],\end{aligned} \tag{71}$$

where $\mathcal{J}_A(s)$ is defined in Eq. (C8), and we have discarded a higher order term of order of $O(l_B)$ in Eq. (71). We remark that the fluctuation contributions to the surface free energy not only consist of the functional determinant, but also a term $[\propto \mathcal{J}_A(s)]$ that arises from the change in the ion distributions near the surface. Note that this term vanishes in both $s\to\infty$ and $s\to 0$ limits. In the latter limit, it can be shown that Eq. (71) reduces to the one-loop surface free energy for the counterion case [44].

IV. DISCUSSION AND CONCLUSION

In conclusion, we have carried out a comprehensive study of fluctuation effects in a charged surface immersed in an electrolyte solution. Using a field-theoretical formulation, we have analyzed analytically the one-loop contributions to the electrostatic potential, ion distributions, and free energies. Our main results may be summarized in the form of a phase diagram depicted in Fig. 11. In the region labeled PB, where $s \ll 1$ and $\Gamma \ll 1$, the system may be approximated by the mean-field PB theory. In the DH region ($s \gg 1$ and $\Gamma \ll 1$), the PB equation can be linearized, leading to an exponential decay of the electric potential with a bare surface charge. On the other hand, $\Gamma > 1/s$, we define a modified DH* regime, where correlation effects are becoming important, and the effective surface charge is substantially reduced. For yet higher Γ, in a region labeled, "charge inversion," the effective surface charge becomes negative and the formation of the second layer of coions occurs. Above the dashed line within the "charge inversion" regime, the electrostatic contribution to the surface tension becomes negative. In the region labeled "SC," denoting the strong-coupling regime, our one-loop calculation would most certainly fail. This regime is delimited by the most upper solid curve in Fig. 11, which is obtained from inspecting the counterion profile when it just becomes negative at some finite distance z. Note that this line represents only an upper bound where our one-loop calculation would break down. As can be seen in Fig. 11, it is reassuring that the charge inversion occurs before the density becomes negative. However, it should be emphasized that there is no guarantee that the one-loop expansion is valid at the point where charge inversion takes place, and the precise location where our one-loop correction breaks down must be given by a higher-loop calculation or by computer simulations.

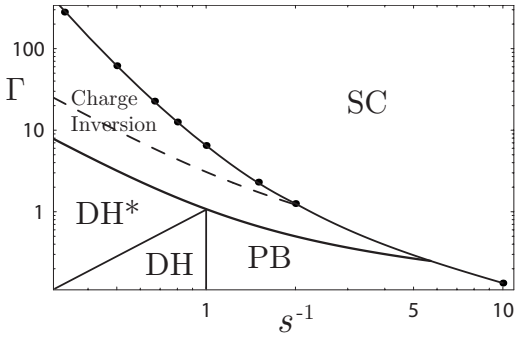

FIG. 11. A phase diagram [$\Gamma \equiv l_B\kappa/(32\pi)$ vs $1/s \equiv l_B n_0/(4Z\kappa)$] for a charged surface immersed in an electrolyte solution. The vertical line separates the Debye-Huckel ($s<1$) and the Poisson-Boltzmann ($s>1$) regimes. The line $\Gamma = 1/s$ further separates a modified DH regime $\Gamma > 1/s$, where the effective surface charge is substantially lowered by fluctuation effects, as compared to the mean-field prediction in the DH regime ($\Gamma < 1/s$). The lower solid curve $\Gamma(s) = -1/\mathcal{A}(s)$ indicates the sign of the effective surface charge just about to reverse. The dashed line signifies the vanishing of the surface tension as determined by Eq. (68). The upper solid line (determined numerically) represents the point at which the counterion profile just becomes negative at some finite distance away from the surface. Thus, SC denotes the strong coupling regime where our one-loop calculation would most certainly fail.

ACKNOWLEDGMENT

The author acknowledges William Kung for his collaborative efforts during the initial phase of this project. This work was supported by NSF Grant No. DMR-0701610.

APPENDIX A: AN ANALYTICAL EXPRESSION FOR THE SELF-ENERGY

In this appendix, we give an explicit expression for the self-energy, Eq. (38). It is convenient to rearrange the expression for $G_s(z,z;q)$ given by Eq. (41) so that the integral over q is manifestly converging. It is straightforward to show that $G_s(z,z;q)$ can be written as

$$\begin{aligned}G_s(z,z;q) = {} & \frac{l_B}{2q^2}\frac{\kappa^2}{\sqrt{\kappa^2+q^2}}\Big\{-\operatorname{csch}^2\kappa(|z|+z_0) \\ & \times[1-(\sqrt{1+s^2}+s)^2\mathcal{M}(q\lambda)e^{-2\kappa|z|(2\alpha-1)}] \\ & + \frac{q^2}{\kappa^2}\mathcal{M}(q\lambda)e^{-4\alpha\kappa|z|}\end{aligned}$$

$$+ 2(2\alpha - 1)\mathcal{M}(q\lambda)e^{-4\alpha\kappa|z|} \coth \kappa(|z| + z_0)\Bigg\}, \tag{A1}$$

where $4\alpha^2 \equiv 1 + q^2/\kappa^2$. Using the expression above, we can explicitly evaluate the self-energy as

$$\beta V_s(z) = \frac{l_B\kappa}{4\pi}\Bigg\{-1 - s[\mathcal{B}(s) + \sqrt{1+s^2}(s+\sqrt{1+s^2})^2\mathcal{J}_1(|z|/\lambda)] \times \operatorname{csch}^2[\kappa(|z| + z_0)] + \frac{\sqrt{1+s^2}}{s}\mathcal{J}_3(|z|/\lambda) + 2\sqrt{1+s^2}\mathcal{J}_2(|z|/\lambda)\coth[\kappa(|z| + z_0)]\Bigg\}, \tag{A2}$$

where

$$\mathcal{B}(s) \equiv \int_s^\infty \frac{du}{u+s}\frac{u(u+s) + 2(u+s)\sqrt{1+s^2} + 2(1+s^2)}{(u+\sqrt{1+s^2})(1+u\sqrt{1+s^2}+u^2)} = (\sqrt{1+s^2}+s)^2\Bigg\{\frac{s^2-1}{\sqrt{s^2-3}}\tanh^{-1}\left(\frac{\sqrt{s^2-3}}{2s+\sqrt{1+s^2}}\right) + \frac{\sqrt{1+s^2}}{2}\ln\left[\frac{\sqrt{1+s^2}(s+\sqrt{1+s^2})^3}{(2s)^4}\right]\Bigg\}, \tag{A3}$$

$$\mathcal{J}_1(x) \equiv \int_s^\infty \frac{du}{u^2-s^2}\frac{1-e^{-2x(u-s)}}{(u+\sqrt{1+s^2})(1+u\sqrt{1+s^2}+u^2)} = \frac{(\sqrt{1+s^2}+s)^2}{2s\sqrt{1+s^2}}\{e^{4sx}E_1(4sx) + \gamma_E + \ln(4sx)\} + 2\{\ln(2s) + e^{4sx}E_1(4sx)\} + \frac{1-s^2}{2\sqrt{1+s^2}\sqrt{s^2-3}}\Bigg\{2\tanh^{-1}\left(\frac{\sqrt{s^2-3}}{2s+\sqrt{1+s^2}}\right) + e^{x(2s+\nu_+)}E_1[x(2s+\nu_+)] - e^{x(2s+\nu_-)}E_1[x(2s+\nu_-)]\Bigg\} - \frac{1}{2}\{\ln[\sqrt{1+s^2}(\sqrt{1+s^2}+s)] + e^{x(2s+\nu_+)}E_1[x(2s+\nu_+)] + e^{x(2s+\nu_-)}E_1[x(2s+\nu_-)]\} - \{\ln(s+\sqrt{1+s^2}) + e^{2x(s+\sqrt{1+s^2})}E_1[2x(s+\sqrt{1+s^2})]\}, \tag{A4}$$

$$\mathcal{J}_2(x) \equiv \int_s^\infty \frac{du}{u+s}\frac{e^{-2ux}}{(u+\sqrt{1+s^2})(1+u\sqrt{1+s^2}+u^2)} = \frac{\sqrt{1+s^2}+s}{\sqrt{1+s^2}}\Bigg\{(\sqrt{1+s^2}+s)e^{2sx}E_1(4sx) - \sqrt{1+s^2}e^{2x\sqrt{1+s^2}}E_1[2x(s+\sqrt{1+s^2})] + \frac{2-s\nu_+}{2\sqrt{s^2-3}}e^{x\nu_+}E_1[x(2s+\nu_+)] - \frac{2-s\nu_-}{2\sqrt{s^2-3}}e^{x\nu_-}E_1[x(2s+\nu_-)]\Bigg\}, \tag{A5}$$

$$\mathcal{J}_3(x) \equiv \int_s^\infty du\frac{e^{-2ux}}{(u+\sqrt{1+s^2})(1+u\sqrt{1+s^2}+u^2)} = e^{2x\sqrt{1+s^2}}E_1[2x(s+\sqrt{1+s^2})] + \frac{\nu_-e^{x\nu_-}E_1[x(2s+\nu_-)] - \nu_+e^{x\nu_+}E_1[x(2s+\nu_+)]}{2\sqrt{s^2-3}}, \tag{A6}$$

$\nu_\pm(s) \equiv \sqrt{1+s^2} \pm \sqrt{s^2-3}$, $E_1(x) \equiv \int_1^\infty dt\, e^{-xt}/t$ is the exponential integral, and $\gamma_E \simeq 0.577216$ is the Euler constant.

APPENDIX B: SOLVING FOR THE ONE-LOOP POTENTIAL

In this Appendix, we present details on solving for the one-loop electrostatic potential leading to Eq. (54). From Eqs. (49) and (52), the final form of the equation that $\langle[\imath\Delta\psi(z)]\rangle_1$ satisfies is

$$\{-\partial_z^2 + \kappa^2 + 2\kappa^2\operatorname{csch}^2\kappa(|z| + z_0)\}\{\langle[\imath\Delta\psi(z)]\rangle_1 = \frac{\kappa^2}{2}G_s(z,z)\sinh\varphi_0(z), \tag{B1}$$

where $G_s(z,z)$ is given by Eq. (40), and we have used the identity $\cosh[\varphi_0(z)] = 1 + 2\operatorname{csch}^2\kappa(|z| + z_0)$. Using Eq. (41) and the identity $\sinh\varphi_0(z) = 2\operatorname{csch}\kappa(|z| + z_0)\coth\kappa(|z| + z_0)$, we find that the solution to Eq. (B1) may be expressed as

$$\langle[\imath\Delta\psi(z)]\rangle_1 = \frac{1}{2}\int\frac{d^2\mathbf{q}}{(2\pi)^2}\frac{l_B\kappa^2}{2q^2}\frac{[-h_1(z) + \mathcal{M}(q\lambda)h_2(z)]}{\sqrt{\kappa^2+q^2}}, \tag{B2}$$

where $h_i(z)$ are the solutions to the inhomogeneous equation

$$\{-\partial_z^2 + \kappa^2 + 2\kappa^2\operatorname{csch}^2\kappa(|z| + z_0)\}h_i(z) = f_i(z), \tag{B3}$$

subject to the boundary conditions that (i) $h_i(z) \to 0$ as $z \to \infty$ and (ii) $\partial_z h_i(z) = 0$ at $z = 0$. In Eq. (B3), $f_i(z)$ are given by $f_1(z) = \operatorname{csch}^3\kappa(|z| + z_0)\coth\kappa(|z| + z_0)$ and $f_2(z) = e^{-4\alpha\kappa|z|}[2\alpha + \coth\kappa(|z| + z_0)]^2\operatorname{csch}\kappa(|z| + z_0)\coth\kappa(|z| + z_0)$. It is straightforward to show that these solutions are given by

$$h_1(z) = \frac{\operatorname{csch}\kappa(|z| + z_0)}{4}\left[\frac{2+s^2}{s\sqrt{1+s^2}} - \coth\kappa(|z| + z_0)\right],$$

$$h_2(z) = \frac{\operatorname{csch}\kappa(|z| + z_0)}{8\alpha}\left[1 + 8\alpha^2 + 2\alpha\left(\frac{2+3s^3}{s\sqrt{1+s^2}}\right)\right] - \frac{\operatorname{csch}\kappa(|z| + z_0)e^{-4\alpha\kappa|z|}}{8\alpha}[1 + 2\alpha\coth\kappa(|z| + z_0)].$$

Using these solutions, we can express $\langle[\imath\Delta\psi(z)]\rangle_1$ as

$$\langle \imath \Delta \psi(z) \rangle_1 = \frac{l_B \kappa}{16\pi} [\mathcal{A}(s) - \mathcal{F}(z)] \operatorname{csch} \kappa(|z| + z_0), \quad \text{(B4)}$$

where $\mathcal{A}(s)$ and $\mathcal{F}(z)$ are defined by and they can be evaluated as

$$\begin{aligned}\mathcal{A}(s) &\equiv \int_0^\infty \frac{s\,dy}{y\sqrt{s^2+y^2}} \left\{ 1 - \frac{2+s^2}{s\sqrt{1+s^2}} + \frac{\mathcal{M}(y)}{2\alpha} \left[1 + 8\alpha^2 + \frac{2\alpha(2+3s^2)}{s\sqrt{1+s^2}} \right] \right\} \\ &= -\frac{2}{\sqrt{1+s^2}\sqrt{s^2-3}} \tanh^{-1}\left(\frac{\sqrt{s^2-3}}{2s+\sqrt{1+s^2}} \right) - \ln\left[\frac{\sqrt{1+s^2}(\sqrt{1+s^2}+s)}{2s^2} \right], \end{aligned} \quad \text{(B5)}$$

$$\begin{aligned}\mathcal{F}(z) &\equiv \int_0^\infty \frac{s dy}{y\sqrt{s^2+y^2}} \left\{ 1 - \coth \kappa(|z| + z_0) + \frac{\mathcal{M}(y) e^{-4\alpha\kappa|z|}}{2\alpha} [1 + 2\alpha \coth \kappa(|z| + z_0)] \right\} \\ &= -s[B(s) + \sqrt{1+s^2}(s+\sqrt{1+s^2})^2 \mathcal{J}_1(|z|/\lambda)] \times [\coth \kappa(|z| + z_0) - 1] - s\sqrt{1+s^2}\mathcal{J}_4(|z|/\lambda), \end{aligned} \quad \text{(B6)}$$

where $\mathcal{J}_1(x)$ is defined in Eq. (A4) and

$$\begin{aligned}\mathcal{J}_4(x) &\equiv \int_s^\infty \frac{du}{u(u+s)} \frac{e^{-2ux}}{(u+\sqrt{1+s^2})(1+u\sqrt{1+s^2}+u^2)} \\ &= \frac{1}{s\sqrt{1+s^2}} \{ E_1(2sx) - e^{2x\sqrt{1+s^2}} E_1[2x(s+\sqrt{1+s^2})] \} + \frac{e^{x\nu_+} E_1[x(2s+\nu_+)] - e^{x\nu_-} E_1[x(2s+\nu_-)]}{s\sqrt{s^2-3}} - \frac{\mathcal{J}_2(x)}{s}. \end{aligned} \quad \text{(B7)}$$

APPENDIX C: DETAILS ON THE EVALUATION OF FUNCTIONAL DETERMINANT

In the appendix, we present the details on evaluating the functional determinant arising from the charged plate $\beta\Delta\Omega_S$. Taking the derivative explicitly with respect to l_B in Eq. (65) through its dependence on κ and λ, we find

$$\frac{1}{\mathcal{A}} \frac{\partial \beta \Delta \Omega_S}{\partial l_B} = \frac{2}{l_B} \frac{\partial \kappa}{\partial l_B} \int \frac{d^2\mathbf{q}}{(2\pi)^2} [\mathcal{I}_1(q) + 2\mathcal{I}_2(q)] - \frac{4}{l_B \lambda^2} \frac{s^2}{\sqrt{1+s^2}} \frac{\partial \lambda}{\partial l_B} \int \frac{d^2\mathbf{q}}{(2\pi)^2} \mathcal{I}_3(q), \quad \text{(C1)}$$

where we have substituted the definition of $G_s(z,z)$, Eq. (40), in Eq. (65), and the integrals $\mathcal{I}_n(q)$ are defined by and evaluated, after inserting the expression for $G_s(z,z;q)$, Eq. (41), and integrating over z, as

$$\begin{aligned}\mathcal{I}_1(q) &\equiv \kappa \int_0^\infty dz G_s(z,z;q) \\ &= \frac{l_B}{2q^2} \frac{\kappa^2}{\sqrt{\kappa^2+q^2}} \left[-\frac{(\sqrt{1+s^2}-s)}{s} + \frac{\mathcal{M}(q\lambda)}{4\alpha s}(s + 4s\alpha^2 + 4\alpha\sqrt{1+s^2}) \right], \end{aligned} \quad \text{(C2)}$$

$$\begin{aligned}\mathcal{I}_2(q) &\equiv \kappa \int_0^\infty dz G_s(z,z;q) \operatorname{csch}^2[\kappa(z+z_0)] \times \left\{ 1 - \left(\kappa z + \frac{s}{\sqrt{1+s^2}} \right) \coth[\kappa(z+z_0)] \right\} \\ &= \frac{l_B}{2q^2} \frac{\kappa^2}{\sqrt{\kappa^2+q^2}} \frac{1}{2s} \left[(\sqrt{1+s^2}-s) - \frac{1}{2\sqrt{1+s^2}} - \frac{\mathcal{M}(q\lambda)}{2\sqrt{1+s^2}} \right], \end{aligned} \quad \text{(C3)}$$

$$\begin{aligned}\mathcal{I}_3(q) &\equiv \kappa \int_0^\infty dz G_s(z,z;q) \operatorname{csch}^2[\kappa(z+z_0)] \coth[\kappa(z+z_0)] \\ &= \frac{l_B}{2q^2} \frac{\kappa^2}{\sqrt{\kappa^2+q^2}} \frac{1}{4s^4} \times [-1 + \mathcal{M}(q\lambda)(1 + 4\alpha s\sqrt{1+s^2} + 2s^2)], \end{aligned} \quad \text{(C4)}$$

where $s \equiv \kappa\lambda$ and $4\alpha^2 \equiv 1 + q^2/\kappa^2$. Inserting these expressions for $\mathcal{I}_n(q)$ in Eq. (C1) and integrating over q, we find

$$\int \frac{d^2\mathbf{q}}{(2\pi)^2} [\mathcal{I}_1(q) + 2\mathcal{I}_2(q)] = -\frac{l_B \kappa}{8\pi} \frac{1}{1+s^2} \int_{s/\sqrt{1+s^2}}^\infty \frac{dy}{y} \frac{1+y}{\frac{1}{1+s^2} + y + y^2}, \quad \text{(C5)}$$

$$\int \frac{d^2\mathbf{q}}{(2\pi)^2} \mathcal{I}_3(q) = -\frac{l_B}{16\pi\lambda} \frac{1}{s^2\sqrt{1+s^2}} \int_{s/\sqrt{1+s^2}}^\infty \frac{dy}{1+y} \frac{2+y}{\frac{1}{1+s^2} + y + y^2}. \quad \text{(C6)}$$

Now, we integrate l_B back to obtain $\beta\Delta\Omega_S$, which can be expressed as

$$\beta \Delta \Omega_S = \frac{\mathcal{A} s^4}{4\pi\lambda^2} \int^s d\theta \frac{\theta^2 \mathcal{J}_A(\theta) + 2\mathcal{J}_B(\theta)}{\theta^5(1+\theta^2)}, \quad \text{(C7)}$$

where $\mathcal{J}_A(s)$ and $\mathcal{J}_B(s)$ are given by

$$\mathcal{J}_A(s) \equiv \int_{s/\sqrt{1+s^2}}^{\infty} \frac{dy}{y} \frac{1+y}{\frac{1}{1+s^2}+y+y^2}$$

$$= \frac{1+s^2}{2} \ln\{(\sqrt{1+s^2}/s)[1+(\sqrt{1+s^2}/s)]\}$$

$$= + \frac{(1-s^2)\sqrt{1+s^2}}{\sqrt{s^2-3}} \tanh^{-1}\left(\frac{\sqrt{s^2-3}}{2s+\sqrt{1+s^2}}\right), \quad \text{(C8)}$$

$$\mathcal{J}_B(s) \equiv \int_{s/\sqrt{1+s^2}}^{\infty} \frac{dy}{1+y} \frac{2+y}{\frac{1}{1+s^2}+y+y^2}$$

$$= - \frac{1+s^2}{2} \ln\left(1+\frac{s}{\sqrt{1+s^2}}\right)$$

$$+ \frac{(3+s^2)\sqrt{1+s^2}}{\sqrt{s^2-3}} \tanh^{-1}\left(\frac{\sqrt{s^2-3}}{2s+\sqrt{1+s^2}}\right). \quad \text{(C9)}$$

Note that in obtaining Eq. (C7), we have to use the fact that $\kappa \sim \sqrt{l_B}$, $\lambda \sim 1/l_B$, and $s \sim 1/\sqrt{l_B}$. Performing the remaining integrals in Eq. (C7), we find

$$\frac{1}{\mathcal{A}}(\beta \Delta\Omega_S) = \frac{1}{4\pi\lambda^2}\left\{\frac{s}{3}\sqrt{1+s^2}(1-2s^2) - \frac{s^2}{2}\ln\left(\frac{\sqrt{1+s^2}}{s}\right)\right.$$

$$+ \frac{1-s^2}{4}\ln\left(1+\frac{s}{\sqrt{1+s^2}}\right)$$

$$\left. + \frac{\sqrt{(1+s^2)(s^2-3)}}{2}\tanh^{-1}\left(\frac{\sqrt{s^2-3}}{2s+\sqrt{1+s^2}}\right)\right\}. \quad \text{(C10)}$$

It is straightforward, but tedious, to verify that differentiating Eq. (C10) with respect to l_B does lead back to Eq. (C1). Combining Eq. (C10) with the surface contribution of the Debye-Huckel term (64), it is straightforward to show that the resulting expression for the surface contribution to $\beta\Delta\Omega$ is given by Eqs. (66) and (67).

[1] J. N. Israelachvili, *Intermolecular and Surface Forces* (Academic Press, San Diego, 1992).
[2] D. Andelman, in *Handbook of Biological Physics*, edited by R. Lipowsky and E. Sackmann (Elsevier, Amsterdam, 1995), Vol. 1, Chap. 12.
[3] W. B. Russel, D. A. Saville, and W. R. Schowalter, *Colloidal Dispersions* (Cambridge University Press, Cambridge, 1989).
[4] F. Oosawa, *Polyelectrolytes* (Marcel Dekker, New York, 1971).
[5] P. Attard, Adv. Chem. Phys. **92**, 1 (1996).
[6] A. G. Moreira and Roland R. Netz, in *Electrostatic Effects in Soft Matter and Biophysics*, edited by C. Holm, P. Kekicheff, and R. Podgornik (Kluwer, Boston, 2001).
[7] A. Y. Groberg, T. T. Nguyen, and B. I. Shklovskii, Rev. Mod. Phys. **74**, 329 (2002).
[8] Yan Levin, Rep. Prog. Phys. **65**, 1577 (2002).
[9] L. M. Varela, M. Garcia, and V. Mosquera, Phys. Rep. **382**, 1 (2003).
[10] H. Boroudjerdi, Y. W. Kim, A. Naji, R. R. Netz, X. Schlagberger, and A. Serr, Phys. Rep. **416**, 129 (2005).
[11] V. A. Bloomfield, Biopolymers **44**, 269 (1998).
[12] T. T. Nguyen, I. Rouzina, and B. I. Shklovskii, J. Chem. Phys. **112**, 2562 (2000).
[13] K. Besteman, M. A. G. Zevenbergen, H. A. Heering, and S. G. Lemay, Phys. Rev. Lett. **93**, 170802 (2004).
[14] J. Pittler, W. Bu, D. Vaknin, A. Travesset, D. J. McGillivray, and M. Losche, Phys. Rev. Lett. **97**, 046102 (2006).
[15] P. Attard, J. Phys. Chem. **99**, 14174 (1995).
[16] J. Ennis, S. Marcelja, and R. Kjellander, Electrochim. Acta **41**, 2115 (1996).
[17] L. Guldbrand, B. Jönsson, H. Wennerström, and P. Linse, J. Chem. Phys. **80**, 2221 (1984).
[18] G. M. Kepler and S. Fraden, Phys. Rev. Lett. **73**, 356 (1994).
[19] J. C. Butler, T. Angelini, J. X. Tang, and G. C. L. Wong, Phys. Rev. Lett. **91**, 028301 (2003).
[20] A. Gopinathan and D. G. Grier, Phys. Rev. Lett. **92**, 130602 (2004); D. Grier and Y. Han, J. Phys.: Condens. Matter **16**, S4145 (2004).
[21] W. Chen, S. Tan, T.-K. Ng, W. T. Ford, and P. Tong, Phys. Rev. Lett. **95**, 218301 (2005).
[22] R. Kjellander and S. Marcelja, Chem. Phys. Lett. **112**, 49 (1984); R. Kjellander and S. Marcelja, J. Phys. Chem. **90**, 1230 (1986); R. Kjellander, T. Akesson, B. Jonsson, and S. Marcelja, J. Chem. Phys. **97**, 1424 (1992).
[23] S. L. Carnie and D. Y. C. Chan, Mol. Phys. **51**, 1047 (1984).
[24] P. Attard, D. J. Mitchell, and B. W. Ninham, J. Chem. Phys. **88**, 4987 (1988); **89**, 4358 (1988).
[25] R. Podgornik and B. Zeks, J. Chem. Soc., Faraday Trans. 2 **84**, 611 (1988); R. Podgornik, J. Phys. A **23**, 275 (1990).
[26] R. R. Netz and H. Orland, Eur. Phys. J. E **1**, 203 (2000).
[27] A. W. C. Lau, D. B. Lukatsky, P. Pincus, and S. A. Safran, Phys. Rev. E **65**, 051502 (2002); A. W. C. Lau and P. Pincus, *ibid.* **66**, 041501 (2002).
[28] D. S. Dean and R. R. Horgan, Phys. Rev. E **65**, 061603 (2002); **68**, 061106 (2003); **69**, 061603 (2004).
[29] B. I. Shklovskii, Phys. Rev. Lett. **82**, 3268 (1999); Phys. Rev. E **60**, 5802 (1999).
[30] A. W. C. Lau, Dov Levine, and P. Pincus, Phys. Rev. Lett. **84**, 4116 (2000); A. W. C. Lau, P. Pincus, Dov Levine, and H. A. Fertig, Phys. Rev. E **63**, 051604 (2001).
[31] R. R. Netz, Eur. Phys. J. E **5**, 557 (2001).
[32] Y. Burak, D. Andelman, and H. Orland, Phys. Rev. E **70**, 016102 (2004).
[33] C. D. Santangelo, Phys. Rev. E **73**, 041512 (2006).
[34] Y. W. Kim and R. R. Netz, J. Chem. Phys. **124**, 114709 (2006).
[35] D. Lacoste, M. Cosentino Lagomarsino, and J. F. Joanny, Europhys. Lett. **77**, 18006 (2007).
[36] L. S. Brown and L. G. Yaffe, Phys. Rep. **340**, 1 (2001).
[37] J. Hubbard, Phys. Rev. Lett. **3**, 77 (1959); R. L. Stratonovitch, Dokl. Akad. Nauk SSSR **115**, 1907 (1957).

[38] M. N. Tamashiro and H. Schiessel, Phys. Rev. E **68**, 066106 (2003).
[39] Luc Belloni, Colloids Surf., A **140**, 227 (1998).
[40] S. L. Carnie and D. Y. C. Chan, J. Chem. Phys. **74**, 1293 (1981).
[41] R. Evans, Adv. Phys. **28**, 143 (1979).
[42] Note that there is an arbitrary constant U_0 in the external potential $\phi(\mathbf{x})$. We have set $U_0=-(2Z)^{-1}\ln(\Lambda_-^{(0)}/\Lambda_+^{(0)})$ in order to correctly produce the free energy for the counterion-only case in Eq. (32) in the limit $\Lambda_-^{(0)}\to 0$. The reason for this is that the counterion-only case and the salt case are in different gauges since that the mean-field potential is zero at the charge surface for the counterion-only case and at infinity for the salt case.
[43] Yi Chen and P. Nelson, Phys. Rev. E **62**, 2608 (2000).
[44] A. W. C. Lau, Ph.D. thesis, University of California, Santa Barbara, 2000.
[45] R. R. Netz, Phys. Rev. E **60**, 3174 (1999).
[46] L. D. Landau and E. M. Lifshitz, *Statistical Physics*, 3rd ed. (Pergamon, New York, 1980).